Neural Computing and Applications (2018) 30:1377–1424
https://doi.org/10.1007/s00521-017-3295-y

REVIEW

Fault detection, location and classification of a transmission line

Debani Prasad Mishra[1] · Papia Ray[2]

Received: 12 December 2016 / Accepted: 22 November 2017 / Published online: 1 December 2017

Abstract
Transient stability is very important in power system. Large disturbances like fault in a transmission line are a concern which needs to be disconnected as quickly as possible in order to restore the transient stability. Faulty current and voltage signals are used for location, detection and classification of faults in a transmission network. Relay detects an abnormal signal, and then the circuit breaker disconnects the unhealthy transmission line from the rest of the health system. This paper discusses various signal processing techniques, impedance-based measurement method, travelling wave phenomenon-based method, artificial intelligence-based method and some special technique for the detection, location and classification of various faults in a transmission network. In this survey, paper signifies all method and techniques till August 2017. This compact and effective survey helps the researcher to understand different techniques and methods.

Keywords Signal processing technique · Artificial intelligence · Classification · Location · Detection · Transmission line

1 Introduction

To supply uninterrupted electric power to the end users is a challenging task for the power system engineers. The cause of the fault may be beyond human control, but it is essential to detect the type of the fault and accurately locate it. Conductors contact with each other or ground, and then fault is generated. Different kinds of faults are single line-to-ground fault (SLG), line-to-line fault (LL), double line-to-ground fault (LLG) and triple line fault (LLL). SLG, LL and LLG faults are unbalanced faults, whereas LLL fault is balanced one. High fault current flows in the power system network due to short circuit, and it causes overheating and mechanical stress on the equipment of the power system [1–5].

Open circuit occurs when any one of the situation aries such as disconnection of one or more phases; or circuit breakers/isolators opens; or joins of cable or jumper break occurs at the tower tension point. Due to open circuit one or two phase, produce unbalance current in the system, so it causes heating of rotating machine. Such abnormal condition should be protected by protective scheme.

Information is collected from journals, books, conference papers, articles online libraries, and databases like IEEE, IET, ELSEVIER, Taylor & Francis, Google Scholar, Scopus, EBSCO and many more relevant websites.

The remaining part of the paper is systematized as follows. Section 2 presents conventional methods that are used for transmission line protection, Sect. 3 is about signal processing technique, Sects. 4 and 5 explain various methods of artificial intelligence (AI)-based techniques and some special techniques, Sect. 6 explains the strength and weakness of all the technique, Sect. 7 is about comparative study of fault classification, location and detection of transmission line, Sect. 8 presents practical case study and comparison of fault detection, classification and location methods, and Sect. 9 gives the conclusion drawn from the survey followed by references.

✉ Debani Prasad Mishra
debani@iiit-bh.ac.in

[1] Department of Electrical and Electronics Engineering, International Institute of Information Technology Bhubaneswar, Bhubaneswar, India

[2] Department of Electrical Engineering, Veer Surendar Sai University of Technology, Burla, India

2 Conventional methods used for transmission line protection

Impedance measurement-based method and travelling wave method are the conventional methods broadly used for detection, classification and localization of the fault in a transmission line [6].

In impedance-based methods, the distance relay operation is accurate and reliable on low value of fault impedance, but did not rely for high fault impedance [7]. Based on a number of current and voltage signals collected from a terminal of transmission line, single-end or two-end impedance methods are proposed. The concept of single-ended impedance-based method is to identify the location of the fault by calculating the apparent impedance seen from one termination of the line. Impedance-based method fault position error is high due to high fault path impedance, load on the line, source parameters and shunt capacitance [8–11].

Two-ended impedance-based method is implemented to locate the fault to eliminate the above-said problems. The disadvantage of this method is a high computational burden due to measurement of current and voltage signals at two ends of the line. However, improve the accuracy to locate the fault [12–14].

Travelling wave-based methods are used to determine the distance of fault by using correlation of forward and backward waves travelling in a transmission line. This method has less error to locate faults in high resistance faults. But the main difficulties are computational burden, expensive and high sampling frequency, difficult for practical application [15–17].

3 Signal processing technique

3.1 Discrete wavelet transform

Time scale decomposition of DWT is done by a digital filtering process up to level 8 as displayed in Fig. 1. The fault signal is fed to the low pass filter (LPF) and high pass filter (HPF) where factor 2 is down-sampled. Detail coefficient ($d1$) is the production of HPF at level one. Approximation coefficient ($a1$) is the production of LPF at level one. Similarly, the process is continued to decompose the signal until and unless only two samples are left for decomposition. Due to less computational burden, DWT is used in fault analysis in a transmission line [18–21].

The DWT of a signal $x(t)$ is defined as

$$\mathrm{DWT}(x,m,n) = \frac{1}{\sqrt{a_0^m}} \sum_m \sum_n x(k)\psi^* \left(\frac{k - nb_0 a_0^m}{a_0^m} \right) \quad (1)$$

where K, m and n are integer. a_0^m and $nb_0a_0^m$ are represented as dilation (scale) and translation (time shift) parameter. b_0 and a_0 are constant and taken as 1 and 2, respectively [89].

3.2 Wavelet transform

Wavelet transform has flexible resizing of the window for use of frequency–time information. It is applicable for non-stationary signal. But detailed information can be obtained in WT at a higher sampling frequency [22–24].

Mathematical expression of a signal $x(t)$ in WT is given below

$$W_{\tau,s}(t) = \frac{1}{\sqrt{s}} \int_{-\infty}^{\infty} x(t)\psi\left(\frac{t-\tau}{s}\right) \mathrm{d}t \quad (2)$$

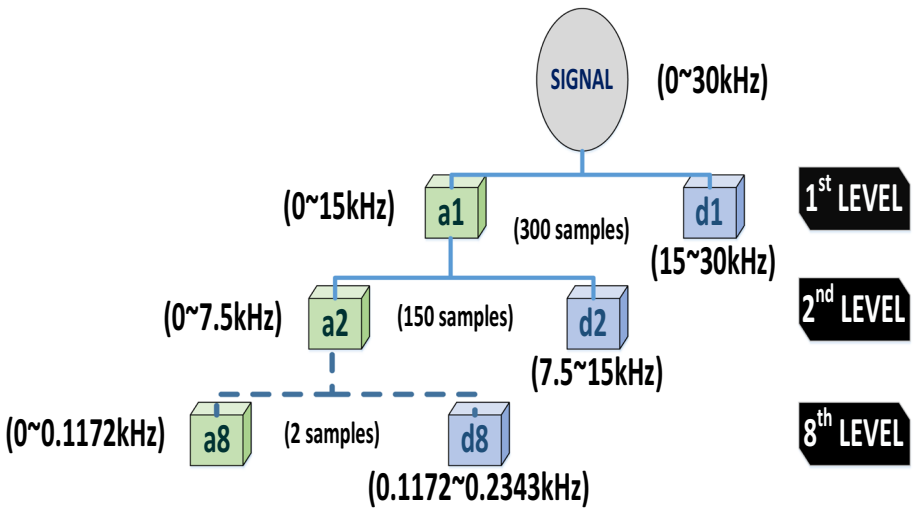

Fig. 1 Decomposition tree of discrete wavelet transform (DWT)

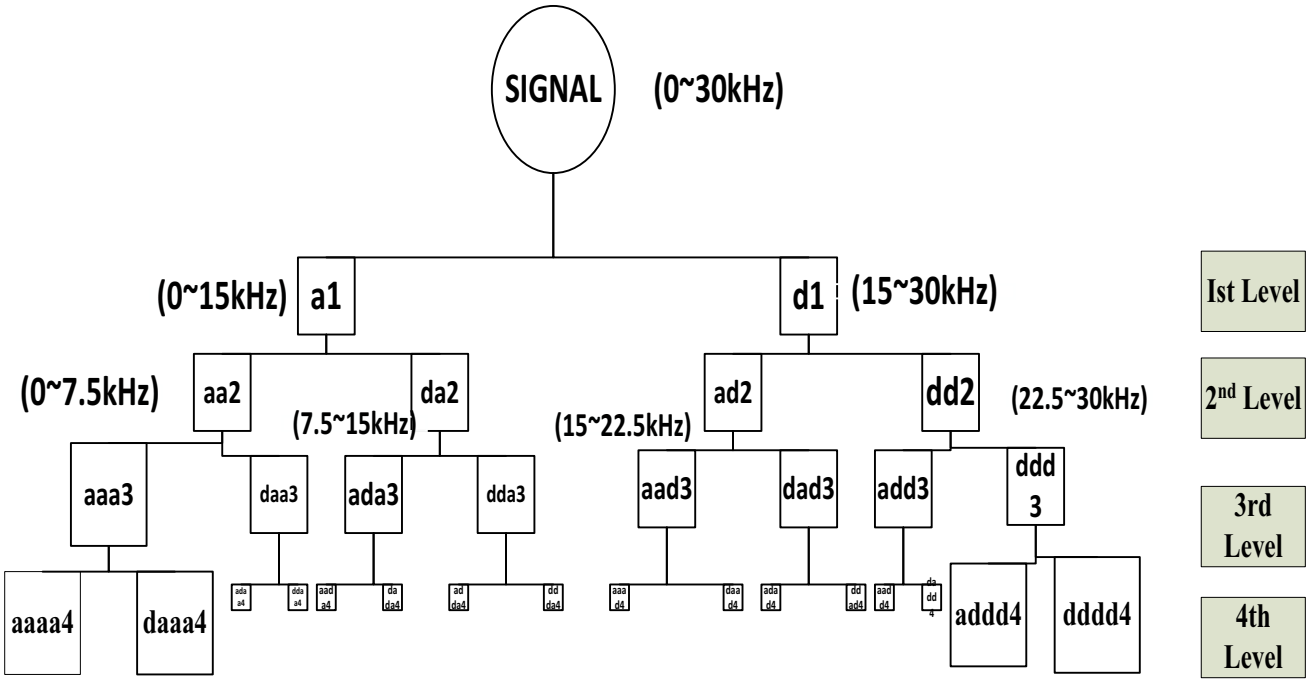

Fig. 2 Wavelet packet transform (WPT)

Translation factor and scale factors are denoted as τ and m, respectively. $\psi(t)$ is the mother wavelet [25].

3.3 Wavelet packet transform (WPT)

To get the important data on high frequency, WPT is implemented. So both approximation coefficient ($a1$) and detail coefficient ($d1$) are decomposed to get full frequency band. Due to calculation burden, it is decomposed up to 4 levels as shown in Fig. 2. So WPT gives an excellent frequency resolution and maximum number of features than DWT [26–28].

WPT of a signal $x(t)$ is

$$W_b^{n,a} = 2^{a/2} \int f(t)\psi_n(2^{-a}t - b)\mathrm{d}t \tag{3}$$

Wavelet position and scale are denoted by b and a. Mother wavelet is ψ_n. The nth and $(n + 1)$th level decomposition are related as

$$W_k^{2n+1,a+1} = \sum h(b - 2k)W_b^{n,a} \tag{4}$$

$$W_k^{2n+1,a+1} = \sum g(b - 2k)W_b^{n,a} \tag{5}$$

where wavelet quadrature mirror filter coefficients are $h(i)$and $g(i)$ [94].

3.4 S Transform

S transform is the combined properties of wavelet transform and short-time Fourier transform (STFT). It is implemented for non-stationary signals where the window width changes inversely with frequency. The main advantage of the ST than other signal processing tool is that it provides information on time, frequency and phase angle of signal. S transform is protected to noise. So it is widely used in fault studies in power system [29–31].

The mathematical expression for S transform [32] for signal $x(t)$ is specified as:

$$S(\tau,f) = \int_{-\infty}^{\infty} x(t)\frac{|f|}{\sqrt{2\pi}} e^{\frac{-(\tau-t)^2 f^2}{2}} e^{-i2\pi ft}\mathrm{d}t \tag{6}$$

Time and frequency signify t and f, respectively. τ is the control parameter for adjusting the Gaussian window. Frequency (f) and phase (ϕ) [32] of the signal is well defined in (7) and (8).

$$\phi(\tau,f) = a\tan\left\{\frac{\mathrm{imag}(S(\tau,f))}{\mathrm{real}(S(\tau,f))}\right\} \tag{7}$$

$$F(\tau,f) = \frac{1}{2\pi}\frac{\partial}{\partial t}\{2\pi f\tau + \phi(\tau,f)\} \tag{8}$$

4 Artificial intelligence (AI)-based techniques

Artificial intelligence (AI)-based methods are used for detection, classification and position of the fault in a transmission network. Support vector machine (SVM), decision

tree (DT) classifier, extremely learning machine (ELM)-based method, artificial immune system (AIS), self-organizing map (SOM), auto-regressive neural network (ARNN), artificial neural network (ANN)-based technique, adaptive neuro-fuzzy inference system (ANFIS), adaptive resonance theory (ARP), fuzzy logic control (FLC) and expert system technique and many more are AI-based techniques used in power system. To find the solution of complex multiobjective nonlinear systems, the above-said methods are used to get faster solution and less error. The paper focuses on signal processing techniques in combination with artificial intelligence methods to accurately detect, locate and classify the faults in a transmission network.

4.1 Artificial neural network (ANN)

Due to simple, better generalization property, adaptive nature, ANN is widely used for fault location, classification and detection in power system transmission line in both real-time and offline application. Faulty signal is trained by ANN as an input and to diagnose fault condition as an output [33].

4.2 Back-propagation neural network (BPNN)

For pattern recognition, BPNN is effectively used. To adjust the feedback of network, error is reduced. The main problem is selecting the number of neurons and hidden layers for each layer. Using large number of neurons and hidden layers makes the training process slow. On the other hand, less number of neurons and hidden layers make divergent of the training process [34] BPNN is used to identify the fault in the transmission network. BPNN and PNN (probabilistic neural network classifier) with S transform are used to detection and classification of fault is proposed in [35]. Six statics features are imported from current or voltage signals by S transform and then classified by probabilistic neural network (PNN). But under noise condition, the accuracy of fault classification is reduced.

4.3 Probabilistic neural network (PNN)

The training examples are classified allowing to their distribution values of probability density function (PDF) in PNN algorithms. Mathematically, the PDF is explained below [36]

$$f_k(X) = \frac{1}{N_k}\sum_{j=1}^{N_k}\exp\left(-\frac{\|X - X_{kj}\|}{2\sigma^2}\right) \tag{9}$$

The output vector of the hidden layer H is modified as

$$H_h = \exp\left(-\frac{\sum_i X_i - W_{ih}^{xh}}{2\sigma^2}\right) \tag{10}$$

$$\text{net}_j = \frac{1}{N_j}\sum_h W_{hj}^{hy} H_h \text{ and } N_j = \sum_h W_{hj}^{hy}, \tag{11}$$

$net_j = \max_k(net_k)$ then $y_j = 1$ else $y_j = 0$. Number of input, hidden units, outputs, training examples and clusters are denoted as i, h, j, k and N, respectively. Smoothing parameter (standard deviation) and the input vector are presented as r and X, respectively. The Euclidean distance between the vectors X and X_{kj} is given below $\|X - X_{kj}\| = \sum_i (X - X_{kj})^2$. The connection weight between the input layer X and the hidden layer H *is* W_{ih}^{xh} and hidden

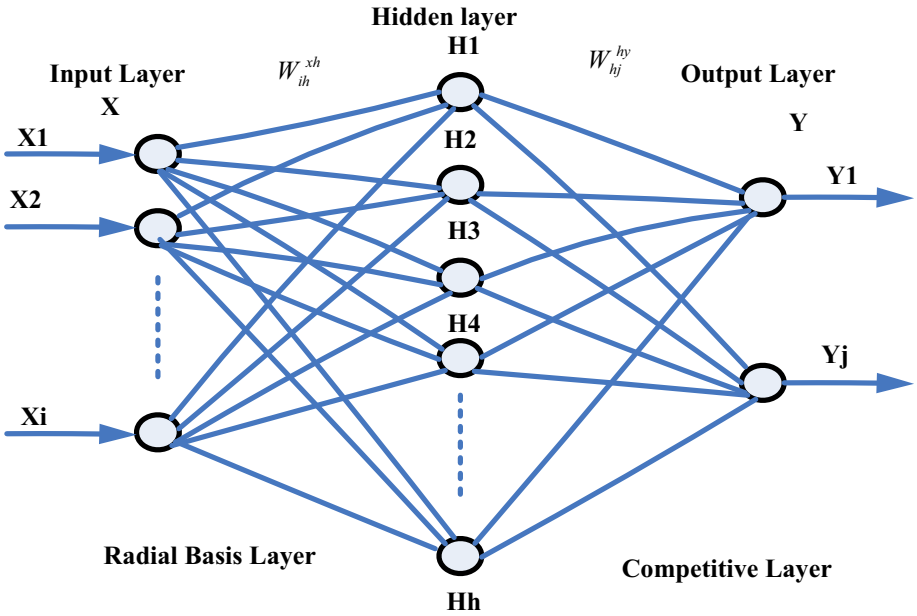

Fig. 3 Structure of PNN

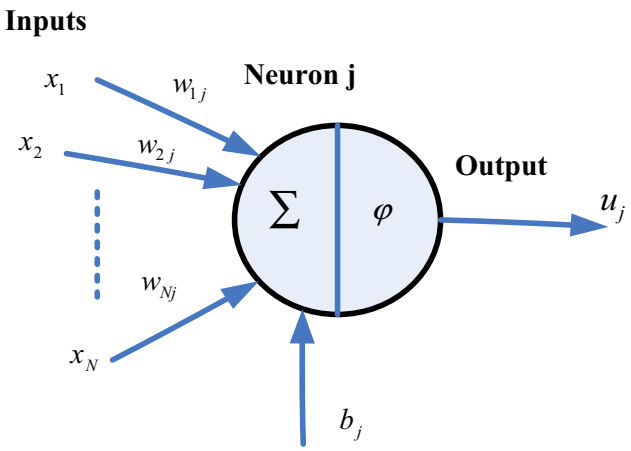

Fig. 4 Feedforward neural network algorithm structure

layer to the output layer Y is W_{hj}^{hy} as shown in Fig. 3 [86].

Input vector is classified into two classes in a Bayesian optimal manner. To calculate the PDF, Bayes decision rule is applied. All PDF is positive and equal to one after integration over all values [86].

4.4 Feedforward neural network (FFNN)

FFNN made with input, hidden and an output layer with multilayer perceptron and back-propagation learning algorithm. The error produced by this method is minimized by adjusting weight and biases of the network. FFNN structure is shown in Fig. 4 [37].

If $x_1, x_2, \ldots, x_i, \ldots x_n$ are the input variable of neuron j. The output u_j is given below

$$u_j = \varphi\left(\sum_{i=1}^{N} w_{ij}x_i + b_j\right) \tag{12}$$

where φ is the activation function and the bias of neuron j is b_j. w_{ij} is the weight factor connecting ith input and jth neuron [168].

4.5 Radial basis function neural network (RBFNN)

RBFNN contains 3 layers, and they are characterized by input, hidden and output layer. The input layer signals are given to the hidden layer where nonlinear radial basis function neuron action will take place, and linear neurons contain the output layer. Figure 5 shows the RBFNN architecture. The output Y is expressed as below

$$Y = f(x) = w_0 + \sum_{i=1}^{m} W_i\phi(D_i) \tag{13}$$

where the x = input vector, bias = w_0, weight parameter = W_i, number of nodes in hidden layer = m, radial basic function (D_i) is a Gaussian function.

$$\phi(D_i) = \exp\left(\frac{-D_i^2}{\sigma^2}\right) \tag{14}$$

where σ is the cluster radius. RBFNN locates the fault in transmission line better than BPNN [38, 39].

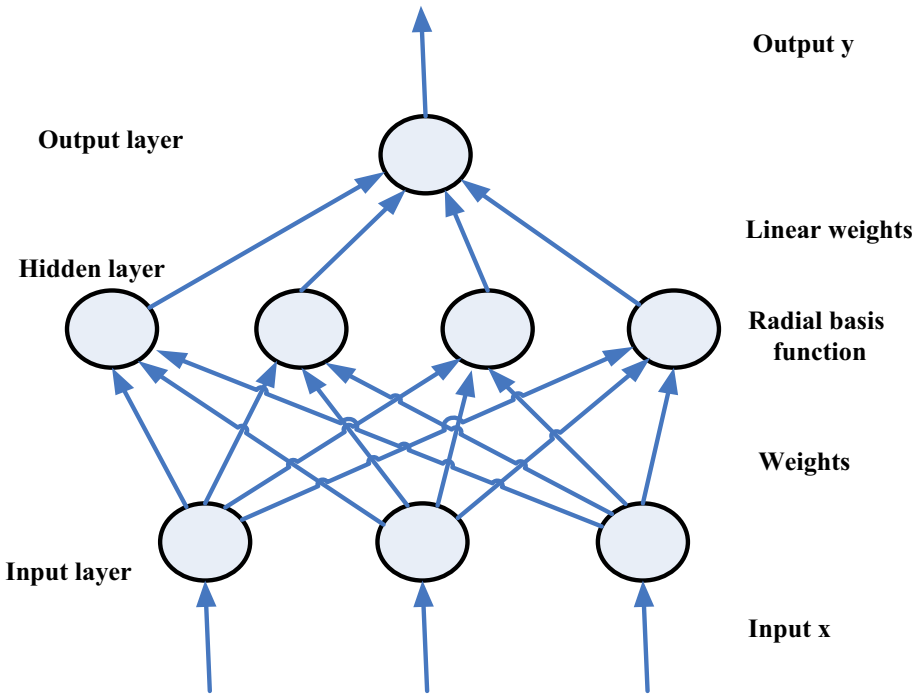

Fig. 5 Architecture of radial basis function network

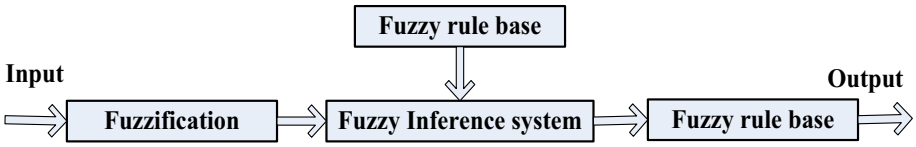

Fig. 6 Fuzzy logic system for fault classification

4.6 Fuzzy logic-based methods

Fuzzy logic works on the principle of 'if–then' relationship. It is used for classification, location and detection of fault in a transmission network. The computational burden of this method is less, but accuracy is affected due to the resistance of the fault and the inception angle of the fault [40, 41].

A simple overall organization of a fuzzy scheme consists of fuzzification, fuzzy inference system, fuzzy rule base and defuzzification as displayed in Fig. 6 for fault classification. In the fuzzification stage, crisp numbers are mapped into fuzzy set. After fuzzification, the fuzzified inputs are given to the fuzzy inference system, and following the given fuzzy rule base, it gives the type of fault in its output. Finally, in the defuzzification stage, the fuzzy output set is mapped into crisp fault type [42].

4.7 Adaptive neuro-fuzzy inference system (ANFIS)

Adaptive network means multilayer network, where every node operates a particular function of the applied data set. The function of the node varies node to node. It is similar to neural network, and the function is same as a fuzzy inference system. ANFIS is used for location and classification fault in a transmission line. Accuracy of this method is better. Due to fuzzy logic, it will take more time to train the data set. A method uses wavelet multiresolution analysis (MRA) to extract the important features, then applying the ANFIS to locate the fault in transmission line [43]. In [44], ANFIS method is compared with the fuzzy inference system (FIS), adaptive neuro-fuzzy inference system and artificial neural network (ANN) to locate the fault in the system. Error analysis by Monte Carlo simulation presents that the ANFIS algorithm is better reliable and precise than FIS and ANN methods in the circumstance of different simulations of various faults. But in this proposed method, computational efficiency is affected during processing of the data and more memory space is required for the calculation.

For fuzzy inference system, x and y are two inputs and fi is the output. Mathematically, 2 fuzzy if–then rules of Takagi–Sugeno's are given below

Rule 1: if x is A_1 and y is B_1, then $f_1 = p_1x + q_1y + r_1$
Rule 2: if x is A_2 and y is B_2, then $f_2 = p_2x + q_2y + r_2$

where fuzzy sets are denoted by Ai and Bi and design parameters are pi, qi and ri.

The architecture of ANFIS consists of 5 layers as shown in Fig. 7 [21].

Layer 1: Every node in these layers is an adaptive node with a node function.

$$o_i^1 = \mu_{Ai}(x) \tag{15}$$

$$o_i^1 = \mu_{Bi}(y) \tag{16}$$

where input to the node are x and y and o_i^1 is the membership function of Ai and Bi. Ai and Bi are the linguistic labels related to node function. So $\mu_{Ai}(x)$ can adopt any bell-shaped function as follows

$$\mu_{Ai}(x) = \frac{1}{1 + \left\{ \left(\frac{x - C_i}{a_i} \right)^2 \right\}^{bi}} \tag{17}$$

Label 2: Every node is fixed and multiplies with the incoming signal. Firing strength is the weight degree of the if–then rules. The output is

$$W_i = \mu_{Ai}(x)\mu_{Bi}(y) \tag{18}$$

Layer 3: It is the normalized layer and normalized the firing strength.

$$\overline{W_i} = \frac{W_i}{W_1 + W_2} \tag{19}$$

Layer 4: All the nodes in these layers are square node with a node function.

$$\overline{W_i} f_i = \overline{W_i}(p_i x + q_i y + r_i) \tag{20}$$

Layer 5: The summation of all incoming signal output is

$$o_i^5 = \sum_i \overline{W_i} f_i = \frac{\sum_i \overline{W_i} f_i}{\sum_i W_i} \tag{21}$$

4.8 Decision tree (DT)

DT is a data miming classification technique. For high-dimensional pattern classification, DT is applied based on selection of attribute that maximizes and fixes data division. Attributes are split into several branches recursively until the termination and the classification are achieved. The mathematically DT technique is

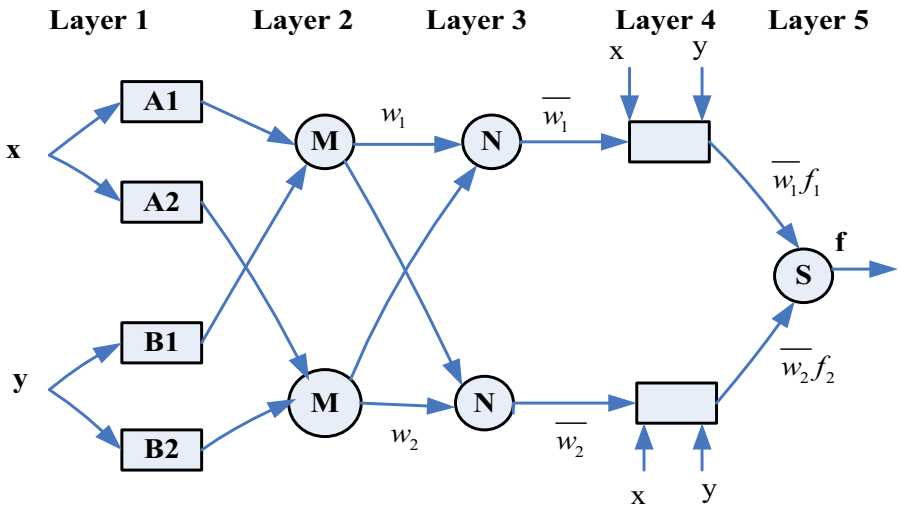

Fig. 7 Structure of ANFIS

$$\begin{aligned} \overline{X} &= \{X_1, X_2, \ldots\ldots\ldots\ldots X_m\}^T \\ X_i &= \{x_1, x_2, \ldots x_{ij}, \ldots\ldots\ldots x_{in}\} \\ S &= \{S_1, S_2, \ldots S_i, \ldots\ldots\ldots S_m\}^T \end{aligned} \tag{22}$$

The available observation number is m, the independent variable number is n, m dimension vector S is having the variable predicated from $\overline{X}$ andX_i. T is the vector transpose. The ith component of n dimension independent variable $x_{i1}, x_{i2}, \ldots x_{ij}, \ldots\ldots\ldots x_{in}$ is autonomous variable of the pattern vector X_i.

The target of DT is to predict S based on the observation of $\overline{X}$. DTs shows differnt level of accuracy when developed from different $\overline{X}$. To get the optimal tree is a difficult task because of the large size of the search space. This algorithm develops a DT by a sequence of local optimal decision about which features can be used to partition data set $\overline{X}$. The optimal size DT T_{k0} is generated according to the below optimization problem

$$R(T_{k0}) = \min_k \{R(T_k)\}, \quad k = 1, 2, 3\ldots\ldots K \tag{23}$$

$$R(T) = \sum_{t \in T} \{r(t)p(t)\} \tag{24}$$

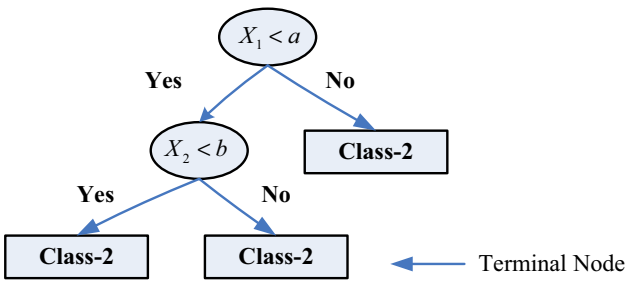

Fig. 8 Binary classification of DT

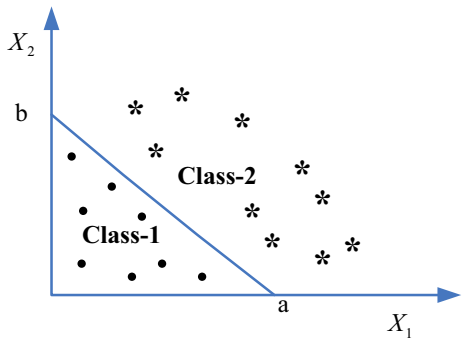

Fig. 9 Boundary-based classification

The misclassification error of the tree T_k is presented by $R(T_k)$, where the optimal DT model T_{k0} is used to reduce the misclassification error $R(T_k)$. Binary tree (T) is $T \in \{T_1, T_2, T_3, \ldots\ldots, T_k, t_1\}$, where the index number of the tree is K, tree node is t, root node is t_1. Re-substitution estimation of error in misclassification of the node t is $r(t)$ and probability drop into node t is $p(t)$. T^L and T^R are denoted as subtrees and define the left and right set of partition. Figure 8 shows the lattice L binary partition into conjointly left/right sets. Two-dimensional binary classifications are shown in Fig. 9. The left set gets the lattice elements with feature q having less value than threshold. In right set, feature q value of lattice components is more than the threshold value [110].

4.9 Support vector machine

SVM is a statistical method used for the computational learning purpose [45]. Sequential minimal optimization (SMO) for kernel support vector machine is implemented in LIBSVM to support the regression (nu-SVR). It has always given a global solution rather than local minima.

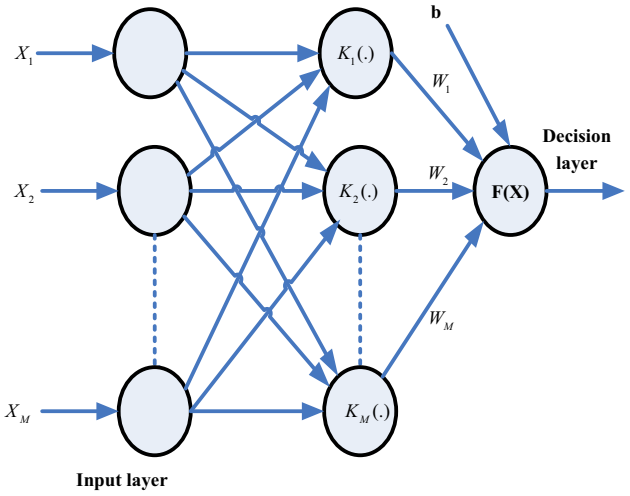

Fig. 10 SVM structure algorithms

The error bound is controlled with cost parameter, and width of hyper axis is controlled by gamma parameter. SVM is used for better accuracy in the location and classification of fault in a transmission line. SVM structure algorithms are shown in Fig. 10, where $K(\cdot)$ = kernel function, M = number of support vectors, $F(x)$ = decision function, W = weights and b = bias [46–48].

For n dimension inputs $Si(i = 1, 2,\ldots M)$, where M is the sample number. Output $Oi = 1$ for class 1 and $Oi = -1$ for class 2.

Mathematically, the hyperplane is

$$f(s) = w^T s + b = \sum_{j=1}^{n} w_j s_j + b = 0 \tag{25}$$

where n dimension vector is w and b is a parameter. The position of hyperplane is decided by w and b magnitude as shown in Fig. 11.

If $Oi = 1$, then the constraints is $f(s_i) \geq 1$ and if $Oi = -1$, then $f(s_i) \geq -1$, so

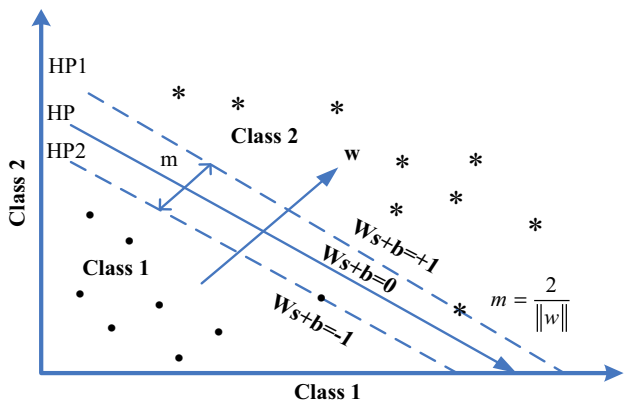

Fig. 11 SVM hyperplane for classification

$$O_i f(s_i) = O_i(w^T s + b) \geq +1 \tag{26}$$

$\|w\|^{-2}$ is the geometrical distance. Then the optimization problem of the optimal hyperplane is [45]

$$\text{Minimize } \frac{1}{2}\|w\|^{-2} + C\sum_{i=1}^{M} \xi_i \tag{27}$$

$$\text{Subject to } O_i(w^T s + b) \geq 1 - \xi_i \text{ and } \xi_i \geq 0 \text{ for } i = 1, 2, \ldots M \tag{28}$$

The optimal bias of b^* is

$$b^* = -\frac{1}{2}\sum_{SV_s} O_i \alpha_i^* (v_1^T s_i + v_2^T s_i) \tag{29}$$

For class 1 and class 2, v^1 and v^2 are random SVM. The decision function is

$$f(s) = \sum_{SV_s} \alpha_i O_i s_i^T s + b^* \tag{30}$$

Data samples have classified as

$$s \in \begin{Bmatrix} \text{Class-1}, & f(s) \geq 0 \\ \text{Class-2}, & \text{otherwise} \end{Bmatrix} \tag{31}$$

4.10 Random forest

Biggest grouping de-correlated tree interpreters are called as random forest, and every tree independently depends on the random vector sample. *Instability* and noise are the major disadvantage of a singular tree, but when developed suitably deep, they have a comparatively small bias. So there are perfect candidates for collaborative rising as they can apprehend complex interactions and totally benefit from a combination-based variance decrease [49]. Random selection of features to divide each node and resampling the training set to propagate each tree yield error rates that are de-correlated and noise tolerant. The errors of the forests are converged to a perimeter as the number of trees in the forest is huge [50].

The main concept of the collaborative tree growing processes is in the n_{th} tree ($n \leq T_{tree}$, total number of tree ensemble). θn is produced as a random vector and independent of $\theta n, \ldots\ldots \theta n - 1$ previous random vector in the same distribution. From the training set M, single tree grows and the attribute set θn, and output classify Sn (Y, θn), here input vector is Y. In the random riven selection, θ contains the number of T_{tree}, the no of attributes $Ta > T_{try}$ in the training set M.

The assemblage of tree-structured classifiers $\{Sn(Y, \theta n), n = 1,\ldots T_{tree}\}$ contained in random forest, where θn is liberated indistinguishable distributed random vectors and tree performs a unit vote for the utmost popular class at input Y, respectively.

All distinct trees are united to predictions for ensemble of trees. For the class that most trees vote is reverted as the extrapolation of the ensemble to classify.

$$c_{\mathrm{RF}}^{T_{\mathrm{tree}}}(Y) = \text{majority vote}\ \hat{C}_n(Y), n = 1\ldots\ldots\ldots n_{\mathrm{tree}} \tag{32}$$

$\hat{C}_n(Y)$ is the class prediction of the nth RF tree.For classification, the class that most trees vote is returned as the prediction of the ensemble. In relatively class frequency, i.e. for prediction probability single tree average is

$$p_{\mathrm{RF}}^{T_{\mathrm{tree}}}\left(c_{\mathrm{RF}}^{T_{\mathrm{tree}}} \in \{M, I\}Y\right) = \frac{1}{T_{\mathrm{tree}}}\sum_{1}^{T_{\mathrm{tree}}} P_{\mathrm{Sn}(\theta n, T)}(c_n \in \{M, I\}|Y) \tag{33}$$

where $P_{\mathrm{Sn}(\theta n,T)}$ is the probability associated with Y by the RF tree Sn(Y, θn). A old-fashioned decision tree basically signifies an overt decision boundary, and a case E is classified into class c if E falls into the decision area consistent to c. The class probability $p(c|E)$ is normally projected by the portion of occurrences of class c in the leaf into which E falls [51, 52].

4.11 Extreme learning machine (ELM)

Extreme learning machine has only one optimize hidden layer. The main advantage of ELM is that there is no requirement of tuning of the hidden layer. Figure 12 shows the structure of ELM. Kernel function and nonlinear activation function are applied to scale the data for a definite range. Weight and bias value adjustment is not required in ELM methods. It is faster and gives better performance than conventional function ELM used for fault location and classification in the power system network [53, 54].

ELM technique is explained by using a training data set of $\{x_i, y_i\}$ where $x_i \in \Re^p$ and $t_i \in \Re^q$, $i = 1\ldots n$. n is the number of samples. Mathematically, single hidden layer feedforward neural network expressed as

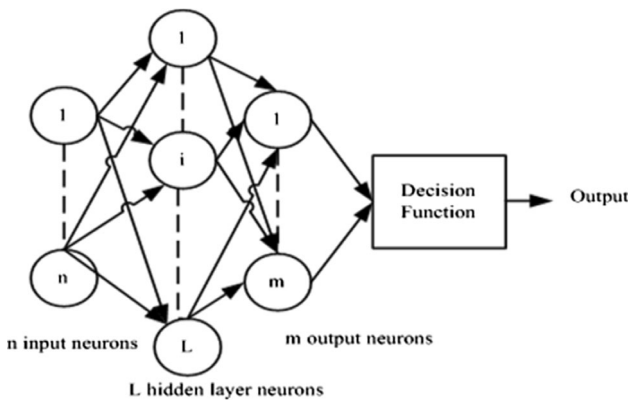

Fig. 12 Structure of ELM

$$\sum_{i=1}^{l} \beta_i f\left(w_i \cdot x_j + b_i\right) = O_{j,j=1,\ldots\ldots\ldots,n} \tag{34}$$

where $f(x)$ *is the* activation function. w_i *is the weight that connects* ith *input neuron to hidden* neuron *and* β_i is the weight that connects ith *hidden* neuron to output neuron. 'b_i' is the bias represented by the threshold of the ith hidden neuron, and output of jth input is denoted by O_j.

For n sample and (L) hidden layer of the ELM is given below [55]

$$\sum_{j=1}^{l} \left\|O_j - t_j\right\| = 0 \tag{35}$$

So, (33) turns out to be:

$$\sum_{i=1}^{l} \beta_i f\left(w_i \cdot x_j + b_i\right) = t_{j,\ j=1,\ldots\ldots\ldots,n} \tag{36}$$

(35) is stated as:

$$H\beta = T \tag{37}$$

where

$$H = f\left(w_i \cdot x_j + b_i\right) \tag{38}$$

H is the hidden layer matrix, and input weight w and biases b are randomly chosen. So least-square solution

$$\min_{\beta}\|H\beta - T\| \tag{39}$$

The result of (36) is stated as:

$$\tilde{\beta} = H^{\dagger}T \tag{40}$$

where $H^{\dagger}$ signifies the Moore–Penrose general inverse of matrix $\boldsymbol{H}$, hidden layer output matrix is symbolized by β and target matrix is symbolized by T.

5 Emerging computational intelligence techniques

5.1 Stationary wavelet transform (SWT)

SWT is alike as WPT and also called as non-decimated wavelet transform. The main change in SWT is up-sampling of the decomposed coefficients. So the filter coefficient at every level holds the same no. of samples as the original signal. DWT does not get the equivalent shift of the output, but SWT has this property due to shifting of the original signal [128]. Filtering and feature extraction by SWT is applied in [130]. Decaying DC offset current due to current transformer, high-order harmonics and noise are removed by SWT.

5.2 Principal component analysis (PCA)

The main advantage of PCA is to map the data from the original high-dimensional space to low-dimensional subspace, so the dimension of the data is reduced, where the best outcome is the variance of the data [145]. In [140] wavelet transform (WT) and principal component analysis (PCA), techniques are used for location and classification faults in Taipower 345 kV power transmission network. For feature extraction, PCA is used in [146].

5.3 Wide-area fault location methods

Location of faults in power network PMU plays a major role, but failure occurs to locate the fault if the end terminal PMU fails to record the faulty signal. It is not economical to locate PMU at every bus of the network due to communication problem and high cost. But optimal PMU placement overcomes this problem [147]. In [148, 149], location of fault in transmission grid was determined using wide-area synchronized voltage measurements with the help of global positioning system (GPS) receivers. The main advantage of the proposed algorithm is, it requires less synchronize measuring devices. The outcomes of the technique give closed-form expression solution. Location of the fault in transmission line by using a non-iterative wide-area technique was proposed in [150]. Impedance matrix was developed by the help of pre-fault positive-sequence and negative-sequence network topology. The location of the fault in the transmission line is determined by using linear least-squares method. The accuracy of the technique is not affected by the high resistance fault. In [151], PMU was used to synchronize the voltage and current signals for the localization of the fault in the transmission grid and successfully diagnose the fault in a hierarchical manner.

5.4 Modal transformation

The phase signal of three-phase systems is decomposed into their modal components by means of the modal transformation matrices. For the un-transposed multiphase lines, eigenvector-based transformation matrix is applied to the phase impedance and admittance matrices to decide the current and voltage transformation matrices. Wedepohl, Karrenbauer and Clarke transformations are non-identical real-value matrices, which are selected for balanced (equally transposed) multiphase lines [135]. In [152, 153], Clarke transformation was implemented to decouple three-phase quantity to α, β (two stationary phase components) and 0 (zero-sequence component) on the basis of characteristics of fault.

5.5 Independent component analysis (ICA)

ICA is defined as given below.

Let random vectors be X and S, where $X = \{x_1, x_2, \ldots\ldots\ldots x_n\}$ and $S = \{s_1, s_2, \ldots\ldots\ldots s_n\}$. The matrix A has element a_{ij}. The X^{T} is the transpose of X a row vector, as all vectors are taken as column vectors. The mixing model is

$$X = As \tag{41}$$

If A is the columns matrix, then A is denoted by a_j. The modified model matrix is

$$X = \sum_{i=1}^{n} a_i s_i \tag{42}$$

The ICA is the statistical model in Eq (40). So ICA is also called generative model [154, 155]. In [156], a combination of ICA, travelling wave and SVM in high-voltage (HV) transmission lines for the location and classification of fault is proposed. The results of the technique give 100 and 99% classification and location accuracy in a real transmission line of a noise faulty signal environment. The main advantage ICA technique overcomes the noise problem in the signal. ICA works on the principle of blind source separation problem [157] and applicable for the separation of the Gaussian signals from non-Gaussian signals [158].

5.6 Pencil matrix method

To extract the parameter from the exponentially damped/undamped signal, PMM is applied in [159]. PMM is less affected by noise and has better computational efficiency [160]. PMM is also used to extract the fundamental frequency component of transmission line and eliminating the DC offset and higher-order harmonic components of the faulty signal [161]. The algorithm of matrix pencil is explained in [162, 163].

6 Strength and weakness of all the technique

Generalized strength and weakness of all the technique are explained in Table 1 as given below.

Table 1 Generalized strength and weakness of all the techniques

Methods	Strength	Weakness
ANN technique	1. ANN is quite successful in determining the correct fault type 2. It is easy to use, with a few parameters to adjust 3. Easy to implement 4. Application of wide range of problems in real life 5. ANN learns and reprogramming is not needed	1. For high-dimension problem, training process is complex 2. Gradient-based back-propagation method gives a local optimum solution for nonlinear separable pattern classification problem 3. Slow convergent in BP algorithm 4. Convergent depends on the choice of initial value of weight parameters connecting to the network
PNN technique	1. No learning process is required 2. No need to set the initial weights of the network 3. No relationship between learning processes and recalling processes 4. It is guaranteed to converge in Bayesian classifier 5. PNN has fast learning time and is insensitive to outlier	1. Required high processing time if the network is large 2. Difficult to know how many neurons and layers are required 3. Learning can be slow 4. Required large memory space to store the model
Fuzzy methods	1. Solve uncertainty problems 2. Using simple 'if–then' type of relation	1. Not robust at all 2. For large training data, experts are required for making fuzzy rules and membership function
ANFIS technique	1. Hybrid learning rule tunes the parameters properly 2. Converges much faster 3. Reduce the dimension of the search space 4. Smoothness and adaptability	1. Computational complexity is very high
SVM technique	1. High accuracy 2. Work well, even if data are not linearly separable in the base feature space 3. Misclassification possibilities are less 4. Maximize the margin to minimize the error bound 5. The dimension of space is not affected by the upper bound generalized error	1. Speed and size requirement both in training and testing is more 2. High complexity and extensive memory requirements for classification in many cases
Random forests	1. Easy to use and simple 2. Accuracy is very high 3. Relatively robust in noise and outliers 4. Not overfitting if taking large no of trees 5. It gives a useful internal estimation of error and correlation 6. Insensitive to the choice of the split	1. The RM model becomes slower for better accuracy as more no. of tree ensembles 2. Random forests become overfit for some data sets with noisy classification/regression tasks 3. Low prediction accuracy and high variance
Decision Tree	1. Simple to understand and interpret 2. Can be combined with other decision techniques 3. Easy to generate rules	1. The calculations can get very complex, particularly if many values are uncertain and/or if many outcomes are linked 2. Information gain in decision trees is biased in favour of those attributes with more levels 3. May suffer from overfitting
ELM technique	1. Only one optimize hidden layer 2. There is no requirement of tuning of the hidden layer 3. Weight and bias value adjustment is not required in ELM	1. Local minima issue 2. Easy overfitting 3. Difficult to find the optimal solution
PCA	1. Minimize the re-projection error 2. It is simple and fast 3. Reduce the dimensionality of the data 4. Reduction of noise	1. If the number of dimensions is greater than the number of data points, then covariance matrix is needlessly large 2. The covariance matrix is problematic to be calculated in a correct manner
Wide-area fault location	1. Both monitoring and control operation are done	1. Placement of PMU in power network is a challenging task for researchers

Table 1 continued

Methods	Strength	Weakness
Modal Transform	1. Independent of frequency and electrical values 2. Single transformation matrix for three-phase system and identical for voltage and current 3. Transposed and non-transposed of the electrical values are done by a simple matrix multiplication without convolution methods	1. It requires a good set of modal parameters 2. This may prove hard to get a complex structure 3. The estimated forces are limited to the frequency range based on the modes nominated for the modal transformation
ICA	1. It minimizes the statistical dependence between its components 2. ICA helps optimal dimension reduction 3. Simplicity of the transformation	1. The order of the independent components (IC) is challenging to define 2. ICA obtained the local minimum solution easily 3. The exact amplitude and sign of the IC cannot be resolved
Pencil Matrix Method	1. The damped harmonic decomposition of percussion signals is recorded 2. PMM is quite robust in the presence of noise 3. Less computational burden	1. The MP method ignores the Hankel structure of the matrix pencil and suffers from a degradation of estimation accuracy at low SNR

7 Comparative studies of fault classification, location and detection of transmission line

To sustain the stability of power networks, it is required to detect the fault and locate the fault in a transmission line. So many methods and techniques are used to detect the faults. Different circumstances like the fault inception angle, loading condition, fault resistance, harmonics and DC offset in the fault signal result in unsatisfactory output. Researchers have implemented various methods and algorithms in both online and offline to identify, locate and classify the faults on transmission network, so that the system operates effectively and efficiently. Comparative analysis of different methods that are used for classification, location and detection of fault in transmission line is shown in the table below. The purpose of the system, input used for algorithm, features and numerical result of the various methods are highlighted in Tables 2, 3, 4, 5 and 6. Table 2 represents the comparative study of fault location of a transmission line, and Table 3 shows the comparative study of fault classification of a transmission line. Fault classification and detection of transmission line is presented in Table 4, and fault classification and location of transmission lines is compared in Table 5. Comparative study of fault classification, location and detection of transmission line is presented in Table 6.

8 Practical case study and comparison of fault detection, classification and location methods

Travelling wave-based technique is implemented in [164] to locate the fault in a 230 kV, 200-km transmission line using the real-time digital simulator (RTDS). The main advantage of this technique is synchronization of data from both the terminal is not required. So this method is applicable for real-time application for synchronized or unsynchronized two-terminal data. The outcome of this method is acceptable. In [165], *PMU-based* state estimation technique is implemented in a real 18-bus distribution network for the detection and location of faults and faulty line. The outcomes of this method are not affected by noise and the nature of load/generators. But this technique is more costly, as PMU is placed at every bus of the system. Current and voltage signals of both ends are used to locate the faults at CEMIG (Energetic Company of Minas Gerais—Brazil) transmission lines in [166]. Digital event recorders are installed for collection of signal. The proposed algorithms mainly depend on the fault point voltage magnitude and do not require the phase angle and synchronized data set. So this technique is robust, accurate and easy to apply in real short-circuit cases. The fault location error is only 0.03%. The *maximal overlap discrete wavelet transform (MODWT)* [167] is applied in real-time detection of fault, where faults are produced by the real-time digital simulator. MODWT has the same characteristic as DWT but upsampling take place there. The current and voltage signals are decomposed by MODWT and then computed for detection of fault in real time. But this technique's accuracy is affected by the saturation of the transducer. In

Table 2 Comparative study of fault location of a transmission line

References	System used	Input used	Post-fault data (Cycle)	Algorithm	Feature	Numerical result
Mazon et al. [56]	Spanish Electrical Power System, 50 Hz/60 Hz La Lomba–Herrera 380 kV, 189.3 km	Pre-fault voltage and current magnitudes	Not mentioned	Artificial neural networks (ANNs	1. The FALNEUR software package uses all these input and output data to train the network 2. The error levels mentioned were achieved with maximum training time varying from 5 s to 2.5 min 3. The architecture selected was the back-propagation method based on the Levenberg–Marquardt optimization technique 4. The 'ansig' function was chosen as transfer function for the hidden layer, and the linear function in the output layer	The average error in the fault distance less than 0.12%, and the maximum error in some situations was not more than 0.7%
Radojević et al. [57]	400 kV, 100 km, 50 Hz	Voltage and current magnitudes	Not mentioned	Least error squares technique	1. The sampling frequency 6400 Hz 2. The duration of data window was 20 ms	The relative error was 0.0099%
Chen et al. [58]	400 kV, 300 km, 50 Hz	Voltage and current of all phases	Not mentioned	Artificial neural network	1. The back-propagation learning rule based on the Levenberg–Marquardt optimization technique is used to train ANN 2. It needs a lot of memory 3. The test data are 2000, and it is trained by 2000 iterations	Maximum absolute error for fault distance is 3.5%
Funabashi et al. [59]	Parallel double-circuit line	Phase voltages and currents signal	Not mentioned	Algorithm-1 employs an impedance calculation and Algorithm 2 employs the current diversion ratio method	1. Phase components of the line impedance are used directly, so compensation of unbalanced line impedance is not required 2. This technique is suitable for the transmission lines for which synchronizing measurement and data transmission systems are available	For balanced line parameters, fault location accuracy < 1.0 km

Table 2 continued

References	System used	Input used	Post-fault data (Cycle)	Algorithm	Feature	Numerical result
de M. Pereira et al. [60]	500 kV, 320 km	Post-fault voltage phasors	Not mentioned	Nelder–Mead simplex (direct search) method	1. The sampling rate used was 960 Hz 2. It does not use post-fault current so the saturation of current transformers error is avoided 3. With and without the equivalent impedance, the error is about 1.5%	An error ± 5% in voltages and currents results in a maximum error of 2.7% of the line length
Liao et al. [61]	200 miles	Voltage signal	Not mentioned	Impedance-based algorithm (IBA)	1. IBA neglects the shunt capacitance of the transmission line and desirable for online applications 2. LPLMBA and DPLMBA are modelling the shunt capacitance 3. CBA is an iterative method to compensate for the shunt capacitance 4. Data synchronization is not needed. 5. It is free of CT errors 6. Compensation-based algorithm (CBA), lumped parameter line model-based algorithm (LPLMBA), and distributed parameter line model-based algorithm (DPLMBA) are more accurate than IBA	Error for all the tested cases is within 1% for IBA and 0.2% for all the other algorithms
Jung et al. [21]	154 kV, combined 14-km transmission line and 6.06-km underground cable	Voltages and current signal	½ cycle	Wavelet transform; Neuro-fuzzy system	1. FIR filter is used to remove the DC offset 2. Mother wavelet—Daubechies (Db4) 3. DWT is decomposed up to level three 4. 228 different faults are generated for analysis 5. Learning is carried out by the back-propagation method	Not mentioned

Table 2 continued

References	System used	Input used	Post-fault data (Cycle)	Algorithm	Feature	Numerical result
Jung et al. [62]	400 kV, 60 km, 50 Hz	Current signal	1 cycle	Wavelet	1. Mother wavelet 'Db5' decomposed up to third level 2. 3840 Hz (64 sample/cycle) was selected for sampling frequency 3. The fault was detected within 1 cycle by using D1 component 4. Fault location by using A3 component of which harmonics are removed	Not mentioned
Reddy et al. [44]	380 kV, 360 km	Voltage and current signal	½ cycle	WPT and ANN	1. Mother wavelet is Daubechies (Db4) 2. The signal is decomposed up to 3 levels by WPT 3. The sampling frequency is 10 kHz 4. It represents a data reduction technique, so computation burden is reduced 5. Pre-fault 1/2 cycle and post-fault 1/2 cycle	Fault location maximum error − 1.67% and min error − 0.06%
Reddy et al. [63]	400 kV, 300-km transmission line	Current signal	Not mentioned	Adaptive neuro-fuzzy inference system, Monte Carlo simulation (MCS)	1. The sampling frequency is 12.5 kHz 2. Daubechies wavelet (Db4) is used as a mother wavelet in multiresolution analysis (MRA) 3. Rules are framed for the FIS editor (Mamdani type) using a fuzzy logic toolbox of MATLAB 4. ANFIS algorithm is quite reliable and accurate in the case of random simulation of the fault	Not mentioned
Perera et al. [64]	230 kV, 12-bus transmission system, 50 Hz	Current signals	Not mentioned	Wavelet transform and travelling wave-based technique	1. DB4 mother wavelet is used 2. The time delay was determined as 0.52 ms 3. Sampling frequency of 50 kHz	Not mentioned

Table 2 continued

References	System used	Input used	Post-fault data (Cycle)	Algorithm	Feature	Numerical result
Ekici et al. [33]	380 kV, 360 km	Current signal	1 cycle	Wavelet packet transform (WPT) and artificial neural network (ANN)	1. Wavelet energy and entropy features are extracted from decomposed signal 2. Daubechies-4 (Db4) was selected as a mother wavelet and decomposed up to 3 levels 3. 2000 data are selected for wavelet packet decomposition 4. The sampling frequency is 10 kHz	Location error less than 2.05%
Sadeh et al. [43]	100-km, 220 kV transmission line combined 90-km transmission line with 10-km underground cable	Fundamental component of three-phase currents and zero-sequence current	1 cycle	Adaptive network-based fuzzy inference system (ANFIS)	1. 2132 patterns are produced for training the ANFISs, among which 1520 patterns are associated with the overhead line and the rest are for the underground cable 2. During training, the maximum percentage error for the overhead line and the underground cable are 0.0109 and 0.031, respectively 3. During testing process, the maximum percentage error for the overhead line and the underground cable is 0.0277 (about 24.9 m) and 0.038 (about 3.8 m), respectively	The exact location of faults such that the maximum percentage error is kept below 0.07%
Gayathri et al. [65]	400 kV and 150-km line, 50 Hz	Positive-sequence voltage and current waveforms	Not mentioned	Radial basis function (RBF)-based SVM and scaled conjugate gradient (SCALCG)-based neural network method	1. The signals are sampled at 5 kHz 2. RBF kernel is selected for the proposed approach 3. The results are obtained in very short duration of time	The maximum error of fault location is limited to 1.93 km to 0.0001 km
Sadeh et al. [66]	400 kV, 300-km transmission line compensated by a series FACTS device	Samples of voltage and current at both ends	Not mentioned	Recursive algorithm	1. Sampling rate of 40 kHz 2. The suggested algorithm does not utilize the compensator device model and the knowledge of the compensator device operating mode to compute the voltage drop during a fault	The error is kept below 0.5%

Table 2 continued

References	System used	Input used	Post-fault data (Cycle)	Algorithm	Feature	Numerical result
Ezquerra et al. [67]	'La Lomba–Herrera' overhead transmission line, 380 kV, 189.3 km, 50 Hz	Pre-fault voltage and current magnitudes at one end	Not mentioned	Artificial neural networks (ANNs) and field-programmable gate array	1. The FPGA platform runs at 60 MHz and consuming less power 2. Hardware implements are done in this technique. 3. ANN executed in the PC with the SARENEUR tool	The fault location error is 0.03%
da Silva et al. [68]	230 kV Transmission System of Tucuruí (TUC 86-3003R-5)	Measurements of voltage and current up to the 50th harmonic	Not mentioned	Neural networks	1. This method uses the harmonic decomposition of the leakage current to analyse the condition of line insulation 2. Use a neural network to locate the fault 3. Determine the capacitance fault value and fault location, help to analyse the insulation conditions of the line.	Not mentioned
Zhang et al. [69]	IEEE 9-bus	Three-phase current and voltage signal	Not mentioned	Pattern classification and linear discrimination principle of pattern recognition theory	1. Wide-area time synchronization capability 2. The running time of discriminant analysis is 0.0320 s. 3. The task of pattern classification is the feature extractor and the classification. 4. Measurement of phasor measurement units.	Not mentioned
García-Gracia et al. [70]	132 kV, 80-km, 50 Hz transmission system	Three-phase current waveform	Not mentioned	Wavelet modulus maxima (WMM) technique.	1. Effective high resistive zero-crossing instant fault detection and location scheme is presented 2. Daubechies-4 (Db4) wavelet was selected as a mother wavelet 3. The sample with 1 MHz (20,000 samples per cycle) to minimize errors in aerial mode measurements 4. Zero mode, velocity is fixed to 2.3205×108 m/s being errors of estimated fault location within 1%.	The maximum relative error detected in these simulations is 0.94%.

Table 2 continued

References	System used	Input used	Post-fault data (Cycle)	Algorithm	Feature	Numerical result
Ray et al. [28]	400 kV, 300 km, 50 Hz series compensated transmission line	Voltage and current signal	1 cycle	WPT and ANN	1. The sampling frequency is 30 kHz 2. Mother wavelet is applied Daubechies (Db2) 3. The signal is decomposed by DWT up to the eighth level 4. Total training data set is 126,000 and test data set is 216,000 6. The feature set is normalized between 0 to 1	Maximum error $< 0.35\%$ and mean error $< 0.25\%$
Jiang et al. [71]	IEEE 39-bus system, ZJP 76-bus system	Current signal	Not mentioned	Phasor measurement unit (PMU) voltage measurements	1. Fault region identification stage and an exact fault location stage are done. 2. The proposed approach is not affected by fault resistance, fault type or pre-fault loading conditions. 3. The constraint of edge-ring circuits for the PMU placement scheme is necessary and is first proposed in this paper.	Max. fault location error 0.8% And location accuracy 100%
Mamis et al. [72]	400 kV, 240 km, 50 Hz	Current signal at one end	Not mentioned	Fast Fourier transform (FFT) and travelling wave theory	1. Time domain signals are sampled at 25.6 kHz with 512 numbers of samples. 2. Hanning window is used to reduce FFT leakage.	The fault location error is reduced to 0.12%
Mahamedi et al. [73]	400 kV, 200-km, 50 Hz double-circuit transmission line	Negative-sequence voltages magnitude	Not mentioned	The ratio between negative-sequence voltages at both ends of the faulted circuit is used to calculate the fault location.	1. It eliminates the errors produced by the CT measurement. 2. It is independent of the fault resistance and fault type 3. The need of synchronization is not required 4. This algorithm could not detect the 3 phase fault	Source reactance's deviate 10% from their real, the estimation of maximum error of 5%.

Table 2 continued

References	System used	Input used	Post-fault data (Cycle)	Algorithm	Feature	Numerical result
Swetapadma et al. [19]	400 kV, 100 km, 50 Hz	Three-phase voltages and three-phase current	Pre-fault one cycle and post-fault 2 cycles	ANN and DWT	1. The cross-country fault is expressed by earth fault presenting in different phases of same circuits at different locations. 2. The percentage of the line covered by zone-1 relay up to 99% 3. Total fault cases—3800 4. ANN is trained using Levenberg–Marquardt algorithm	Percentage error in fault location is within ± 1% in
Gayathri et al. [39]	400 kV, 150-km, EHV double-circuit transmission line	Three-phase Positive-sequence voltage and 6 line current	Not mentioned	Radial basis function (RBF)-based SVM and scaled conjugate gradient (SCALCG)-based neural network method	1. Sampling rate is 5 kHz 2. Very short duration of time (2e−004 s) to locate the fault. 3. Mutual coupling between the lines problem is overcome. 4. RBF kernel is used for extraction of the principle eigenvectors of the feature space and de-noising the signal.	The maximum errors of fault location 1.852 km (double circuit) and minimum—7.874e−003 km
Dobakhshari et al. [74]	Western systems, coordinating council (WSCC)9-bus and 22-bus test systems 345 kV	Positive-sequence voltage	Not mentioned	Linear-weighted least-squares (WLS) method	1. Sampling rate is 100 kHz 2. The proposed method is not affected by fault type and resistance 3. This technique is obviating the need to deal with CT saturation as well as unreliable zero-sequence parameters of the line.	Fault location error is less than 1%
Capar et al. [6]	380 kV, 300-km, transmission line with series capacitor	Voltage and current signal	Not mentioned	Impedance based	1. Test system simulated in DIgSILENT 2. Sampling rate is 10 kHz 3. Simulation time was 0.2 s	Fault location error is less than1%

[169], maximal overlap discrete wavelet transform (MODWT) and discrete wavelet transform (DWT) are implemented in real time for fault detection and location 500 kV, 400-km-long transmission lines. The MODWT gives acceptable accuracy (mean error is 0.63%) as comparable to DWT. The technique is executed with the help

Table 3 Comparative study of fault classification of a transmission line

Reference	The system used	Input used	Post-fault data (Cycle)	Algorithm	Feature	Numerical result
Dalstein et al. [75]	380 kV, 100-km double-line transmission line	Three-phase voltages and currents	Not mentioned	Feedforward neural networks (FNN)	1. 1 kHz sample rate is used 2. 30 input nodes, two hidden layers and an output layer with 11 nodes 3. 45,000 training patterns simulating and 30000 for training patterns	Longest classification time is 7 ms
Song et al. [76]	Not mentioned	Three-phase voltages and currents	Not mentioned	The back-propagation neural network structure with supervised learning	1. The neural networks concerned here include: (i) back-propagation net; (ii) features-map net; (iii) radial basis function net; (iv) counter-propagation net and (v) learning vector quantization net (LVQ) 2. Total 55 000 patterns are generated 3. A data window length of 4 samples at 720 samples/second	The maximum misclassification rate is 0.04% of LVQ network
Aggarwal et al. [77]	Double-circuit transmission lines 128 km, 5 GVA and 35 GVA generation	Three-phase voltage and six-phase currents	Not mentioned	Back-propagation network classifier	1. It is used as a front end to an output layer with supervised learning and is called self-organizing map (SOM). 2. SOM is a combined unsupervised/supervised learning network 3. Sampling rate (800 Hz) and 3 sample-data window gives satisfactory results 4. The number of Kohonen neurons is very much dependent on the number of training sets	Misclassification rate SOM-based network was less than 1%
Whei-Min Lin et al. [78]	80 km, S1-24GVA, S2-19SVA	3 voltages and 3 currents	Not mentioned	Radial basis function (RBF) neural network with orthogonal-least-square (OLS) learning	1. Gaussian function was chosen for RBF 2. The sampling rate of 800 HZ 3. The network based on a BP training algorithm 4. Hidden layer possesses 20 neurons and converged after 85 049 epochs	Not mentioned

Table 3 continued

Reference	The system used	Input used	Post-fault data (Cycle)	Algorithm	Feature	Numerical result
Adu et al. [79]	Southwestern Public Service Company (SPS), Companhia Energetica de Minas Gerais (CEMIG) in Brazil,	Positive- and negative-sequence components of the current parser	Not mentioned	The algorithm is based on the measurement of phase angles between the positive- and negative-sequence components of the current phasor	1. It can be used where multiple transmission lines are present 2. The proposed technique is independent of the isolation device, system configuration, and the power system operating conditions during faults 3. Selecting the faulted feeder by using the least error squares phasor estimator 4. Fault data provided by Ontario Hydro and Companhia Energetica de Sao Paulo (CESP) in Brazil	Not mentioned
Pradhan et al. [37]	230 kV, 200-km, 50 Hz series compensated line	Current signal	Not mentioned	Discrete wavelet transform and fuzzy logic system	1. Mother wavelet is Meyer 2. 90% of the line is simulated at 0.02 s 3. Triangular fuzzy membership is applied 4. Two FLS designs for faulty phase/ground selection and fault section identification	Not mentioned
Youssef et al. [80]	300-km, 50 Hz transmission lone	Three line current	Not mentioned	Wavelet transforms and fuzzy logic-based technique	1. The sampling rate is 4.5 kHz 2. Db8 mother wavelet is used 3. Wavelet is decomposed up to level four 4. This paper represented online application of fault classification 5. This method is fast, accurate, robust and simpler computation	Identify the faults in less than 10 ms
Das et al. [81]	400 kV, 300 km, 50 Hz	Three line current	½ cycle	Fuzzy logic	1. Implement a digital distance protection scheme 2. 2400 test cases are studied 3. The time taken by this method is about 10 ms	The accuracy is more than 97%
Megahed et al. [82]	500 kV, 50 Hz, 300 km power system	Three phases and ground current signal	½ cycle	Discrete wavelet transform	1. The mother wavelets used 'Db4' for fault-zone identification and 'Haar' for fault classification 2. The sampling frequency is taken as 200 kHz	Not mentioned

Table 3 continued

Reference	The system used	Input used	Post-fault data (Cycle)	Algorithm	Feature	Numerical result
Mahanty et al. [83]	400 kV, 100 km	Three-phase currents	Not mentioned	RBF neural network and wavelet	1. Wavelet multiresolution analysis (MRA) level 1 2. The sampling interval being 10 μs 3. Analysing wavelet is biorthogonal spline 4. FIA range 0°–360°	Not mentioned
Mahanty et al. [84]	400 kV, 300 km, 50 Hz	Three-phase currents	½ cycle	Fuzzy logic	1. The sampling interval is 1 ms and the number of samples per phase is ten 2. The triangular fuzzy membership function is used and varies from 0 to 1. 3. The sampling interval for the proposed method is 1 ms	Not mentioned
Samantaray et al. [85]	230 kV, 50 Hz, 300 km TCSC is located at the midpoint, 150 km	Three-phase currents signal	1 cycle	S transform and probabilistic neural network (PNN)	1. S transform is an extension to the idea of the Gabor transform and wavelet transform 2. It is based on a moving and scalable localizing Gaussian window 3. Sampling rate of 1 kHz 4. Energy and standard deviation are the features to extract for analysis 5. Out of 500 data sets generated, 300 data sets are used to train and 200 for testing	Maximum classification accuracy is 98.62% and section identification is 99.86%
Samantaray et al. [86]	400 kV, 300 km, 50 Hz	Post-fault current and voltage samples	1/4 cycle	Support vector machine (SVM)	1. The total time taken for faulty phase selection is 10 ms (half-cycle). 2. Sampling frequency of 1.0 kHz 3. SVM 1 and SVM 2 trained and tested with 300 data sets for phase selection and ground detection, respectively 4. The polynomial and Gaussian kernels-based SVMs are used	Faulty phase selection and ground detection with error $< 2\%$.

Table 3 continued

Reference	The system used	Input used	Post-fault data (Cycle)	Algorithm	Feature	Numerical result
Valsan et al. [87]	50 Hz	Three-phase currents signal	1/3 cycle	Field-programmable gate array (FPGA).	1. Test work is done with very high-speed integrated circuit (VHDL) 2. The sampling frequency is 2 kHz 3. Daubechies (Db6) wavelet is used 4. Total of 3520 test cases were generated 5. Karrenbauer transformation used avoids the need for multipliers	The fault classification time is 6 ms and gives 100% accurate results
Nguyen et al. [88]	500 kV. 20 miles, 60 Hz	Three-phase currents signal	1 cycle	Adaptive neuro-fuzzy inference system	1. Seven inputs with two membership functions, so a 128 rules system 2. The sampling frequency is 30,240 Hz 3. 2660 fault cases for training data 4. The main advantage of ANFIS is automatically tuning the fuzzy membership functions	Classification accuracy more than 99.92% and in real time more than 81.82%
Upendar et al. [89]	400 kV, 50 Hz, 300 km	Three-phase current signals	Not mention	PSO-based multilayer perceptron neural network and wavelet transform	1. Current signals are being decomposed into nine levels using the MRA algorithm 2. Current signals with 512 samples 3. Daubechies mother wavelet is used 4. 48 960 training samples are 1209 600, and testing data sets are generated	99.91% Average fault classification accuracy
Pérez et al. [24]	500 kV, 390 km, 50 Hz	Current signal one of the phases	1/10 cycle	Adaptive wavelet algorithm (AWA) and Bayesian classification	1. Sampling rate is 500 kHz 2. 546 fault cases 3. Daubechies (Db4) mother wavelet is used 4. ATA windows of approximately 2 ms are required	Accuracy is 100%
Chothani et al. [90]	400 kV,	Current signal	1 cycle	Support vector machine (SVM)	1. 28 800 fault cases are used 2. Accuracy of 99% for all the fault cases 3. Effect of CT saturation is taken into consideration	The Gaussian RBF kernel gives the highest accuracy of 99.833%

Table 3 continued

Reference	The system used	Input used	Post-fault data (Cycle)	Algorithm	Feature	Numerical result
Seyedtabaii et al. [91]	230 kV, 200 km, 50 Hz	Phase currents	1 cycle	Artificial neural network (NN)	1. The sampling rate is 20 samples per cycle 2. 1260 faulty cases were simulated using MATLAB-Simulink 3. Signal sampled at 1 kHz 4. Accurate MLP training without any heuristic parameter involvement and reduce the size of the network to the minimum of one node per phase	Not mentioned
Beg et al. [92]	132 kV network with 14 buses and 10, 14 bus are 220 kV lines, 50 Hz	Voltage signal	3 cycles	Discrete wavelet transforms and feedforward artificial neural network	1. MRA wavelet decomposition up to level 5 and bior1.3 is used as the mother wavelet 2. 262 non-fault and 448 fault events are produced using PSCAD/EMTDC 3. 80% data are given for training 4. Network contains one input layer, two hidden layers and one output layer	Overall classification accuracy of 96.79%
Jafarian et al. [93]	230 kV, 330 km	Current signal	1/4 cycle	Dyadic wavelet transform and support vector machine (SVM)	1. The sampling frequency of 160 kHz 2. The signals are decomposed up to five stages 3. 1500 fault cases were simulated 4. 800 faults were randomly selected to train the SVMs, and the remaining cases were used to test the trained SVMs 5. The wavelet transform is used to remove random noise	Maximum classification accuracy is 100% of Gaussian kernel function
Vyas et al. [94]	400 kV, 300-km, a TCSC is placed at midpoint of the transmission line	Current signal	½ cycle	Polynomial-based Chebyshev neural network (ChNN) and discrete wavelet packet transform (DWPT)	1. Fault patterns are produced by PSCAD 2. Training data—2400 Testing data—30,000 3. Sampling frequency—4 kHz 4. Suitable for digital protection application 5. Faster and more accurate	Accuracy—99.39%

Table 3 continued

Reference	The system used	Input used	Post-fault data (Cycle)	Algorithm	Feature	Numerical result
He et al. [95]	500 kV, 50 Hz	Three-phase current signals	¼ cycle	Wavelet transforms and rough membership neural network (RMNN) classifier	1. Back-propagation (BP) algorithm is employed for determining the optimal connection weights between neurons of the different layers in the RMNN 2. The sampling frequency is 50 kHz 3. Mother wavelet is Daubechies (Db4) 4. Classification rate is 100% for non-ground fault and 97% of ground fault	Average success classification rate of 99.4%
Vyas et al. [96]	300 km, 50 Hz, three-phase, 400 kV and TCSC at the middle of the transmission line	Three-phase current signals	1/2 cycle	Discrete wavelet transform (DWT) and Chebyshev neural Network (ChNN).	1. 3600 fault patterns are separated out for training and remaining 28,800 fault patterns are explicitly used for testing of the algorithm 2. The sampling frequency is 4 kHz 3. Here 'Db1' used as a mother wavelet and decomposes up to the first level of resolution	Classification accuracy is above 99%
Gao et al. [97]	300-km, 345 kV,	Positive-sequence three-phase voltages	1 cycle	Classification and regression tree (CART) algorithm	1. CART is a nonparametric decision tree learning technique that is in the form of if–else statements 2. Total number of fault cases—2880	Learning accuracy—100% Testing accuracy—99.981%

of real-time digital simulator (RTDS). Real-time and off-line fault classification is done in [170] by using the MODWT technique in 230 kV transmission line. Offline and real-time classification are evaluated by using actual oscillographic records and real-time digital simulator (RTDS), respectively. For line-to-ground and line-to-line faults, the classification accuracy in real time is 100%. But in the wavelet coefficient energy investigation, the mis-classification problem occurs for the double line-to-ground fault. In [136], hardware arrangement is done for analysis

Table 4 Comparative study for classification and detection of fault on a transmission line

Reference	System used	Input used	Post-fault data (cycle)	Algorithm	Feature	Numerical Result
Barros et al. [98]	Different lines of the power system of northern Spain	Voltages of the three phases	Not mentioned	Kalman filters and 8-bit microprocessors	1. Low-cost 8-bit 6809-type processors 2. Fault detection by Kalman filters 3. An 8-bit MC6809B processor, which operates with a 2 MHz clock 4. Three-phase faults are correctly detected in the first two samples analysed 5. Used in computer relaying applying 6. 5 cycles of the pre-fault and 150 cycles post-fault signals	Classification and detection of faults accurately less than 20 ms
Liang et al. [99]	174.4 km	Current and voltage signals	Not mentioned	Wavelet multiresolution analysis (MRA)	1. Sampling frequency of 600 Hz and a single-stage MRA filter bank are selected 2. Daubechies (Db4) wavelet is used 3. MRA gives a reliable solution in high impedance fault condition	Not mentioned
Chowdhury et al. [100]	Transmission line modelled using Simulink having three segment model	Three-phase voltages and currents signal	Not mentioned	Wavelet theory and artificial neural networks for detection and Kohonen network for classifying the fault	1. Creation of a measure to serve as the indicator of normal–abnormal behaviour and 2. Design of a decision rule, based on that measure, to detect the fault 3. Three-layer feedforward neural network is used for fault detection 4. Use Daubechies wavelet of order ten	Not mentioned
Wang et al. [101]	Simulation is done using EMTDC/PSCAD program	Faulted voltage and current	1 cycle	Fuzzy neuro-techniques	1. Back-propagation algorithm and a suitable fuzzy controller 2. FFT algorithm removes the high harmonic components and attenuates the exponential component	The detection is achieved in less than 10 ms

Table 4 continued

Reference	System used	Input used	Post-fault data (cycle)	Algorithm	Feature	Numerical Result
Hong et al. [102]	220 kV, 177.4 km	Three-phase currents	Not mentioned	B-spline wavelet transforms	1. Sampled at a frequency of 600 Hz, so the computation burden decreased 2. It is suitable for the high-speed digital distance protection 3. By comparing the moving average of these transforms, fault types are easily classified 4. This algorithm is valid for any fault inception angle	Not mentioned
Dash et al. [103]	190 miles, 50 Hz	Voltage and current signal	Not mentioned	Minimal radial basis function neural network (MRBFNN).	1. This technique uses a sequential learning procedure to determine the optimum number of neurons in the hidden layer without resorting to trial and error 2. The number of training patterns is reduced to just 40 for fault classification and 70 for location task, respectively 3. LIKF (locally iterated Kalman filter) is used to adjust the network parameters like centre, width and connecting weight	Not mentioned
Martín et al. 2003 [104]	300 km, 50 Hz	Three-phase voltages and currents signal	¼ cycle	Discrete wavelet transforms (DWTs) and ANN	1. The sampling frequency is 1600 Hz 2. Two hidden layers and feedforward neural networks are used 3. A total of 3800 simulations was generated half of them were used for training, and the other half for testing 4. Haar and Daubechies wavelets are used	Not mentioned

Table 4 continued

Reference	System used	Input used	Post-fault data (cycle)	Algorithm	Feature	Numerical Result
Yeo et al. [105]	154 kV Korean transmission line, 26 km	RMS value of three-phase currents and zero-sequence current	½ cycle	Adaptive network-based fuzzy inference system (ANFIS)	1. Sampling rate of 64 samples per cycle 2. Trapezoid function is used as membership function 3. Detect and classify the fault type in a transmission line based on the RMS value of phase currents and zero-sequence current 4. The fault is detected to just 18 samples, i.e. about a quarter cycle of the fundamental frequency	Maximum classification error of 2.81%
Chanda et al. [106]	400 kV, 300 km, 50 Hz	Three-phase currents	Not mentioned	Wavelet multiresolution analysis (MRA)	1. Daubechies eight (D-8) wavelet transforms decomposed up to 3 levels 2. Signals are sampled every 80 microsecond 3. Simulation is carried out by using fault inception angle 0°–180° and high impedance faults of 500 O	Not mentioned
Chanda et al. [107]	230 kV, 200 km, 50 Hz	Current in each phase	Not mentioned	Wavelet multiresolution analysis	1. Wavelet multiresolution analysis Daubechies (D-8) wavelet transforms decomposed up to third level 2. Sampling frequency of 12.5 kHz	Not mentioned
Silva et al. [20]	230 kV, 188 km, 60 Hz	Voltage and current waveforms	1 cycle	Discrete wavelet transforms and artificial neural networks (ANNs)	1. Sampling frequency—1200 Hz 2. Normalization current and voltage signal − 1 to 1 3. Mother wavelet uses Daubechies-4 (Db4) 4. Number of iterations is 426 5. Number of cases is 720 6. Minimum root-mean-square (rms) error is 0.02	Fault classification accuracy is 99.83% and fault detection is 100%

Table 4 continued

Reference	System used	Input used	Post-fault data (cycle)	Algorithm	Feature	Numerical Result
Aguilera et al. [108]	500 kV series compensated transmission line, 400 km	One-phase voltage signals	1 ms	Discrete WT	1. Simulated with MICROTRAN and MATLAB 2. Classification between single phase-to-ground fault and other faults, the mother wavelets sym7 and Db15 for detail-3 and detail-8 is used and sym8 and coif5 for ungrounded faults 3. Sampling frequency of 80 kHz 4. Spectral energy (SE) is used as features	Operating time of less than 4 ms
Zhang et al. [109]	500 kV, 200 miles, 50 Hz	Three-phase voltage and current signals	½ cycle	Wavelet transform and self-organized art neural network algorithm	1. The sampling rate of 200 kHz 2. This method is used to classify internal and external faults 3. Adaptive resonance theory (ART) neural network is used and the number of clusters is increased and their positions are updated automatically during the learning 4. The signals are decomposed using Db5 wavelet to level 5 5 Generated a set of 3960 fault scenarios for the system	Fault detection accuracy = 99.7% for single line, 92% of parallel line, fault classification accuracy = 99.65%
Valsan et al. [22]	400 kV, 4 bus, and L1, L2, L3, and L4 transmission lines of length 150, 200, 240, and 180 km, respectively	Phase current signal	Not mentioned	Multiresolution wavelet analysis	1. Db6 mother wavelet is used 2. Total number of test cases—3600 3. Karrenbauer transformation that is used avoids the need for multipliers 4. Sampling frequency—20 Kz	Fault classification accuracy—100% for LG, LL and LLL fault. For LLG fault classification accuracy—99.44%

Table 4 continued

Reference	System used	Input used	Post-fault data (cycle)	Algorithm	Feature	Numerical Result
Samantaray et al. [110]	230 kV, 50 Hz, TCSC is placed at midpoint of the 300-km transmission line	Three-phase current and voltage signal	1 cycle	Decision tree (DT) and SVM	1. TCSC is designed, so it provides 30% compensation at 180° (minimum) and 40% compensation at 150° (maximum) firing angle 2. Noisy environment is taken into consideration 3. The sampling frequency is 1.0 kHz 4. 70–30% training and testing data sets 5. Fault cases simulated for TCSC line are 16,800 and for UPFC 25,600 6. The computational burden of SVM is higher compared to DT	The classification accuracy for SVM and DT is 93.6 and 98.8%, respectively,
He et al. [111]	500 kV, 300 km, 50 Hz	Zero-sequence current and voltage signal	½ cycle	Wavelet singular entropy (WSE)	1. Sampling frequency—20 Kz, 2. The model is established in EMTDC/PSCAD 3. Detected fault time by WSE 200.001 ms 4. No of tests—20 5. The 'db4' mother wavelet and 4-scaled WT are chosen	Classification overall accuracy—100%
Yusuff et al. [112]	400 kV, 361.65 km, 50 Hz	Voltage and current signal	¼ cycle	SVM and fuzzy logic reasoning (FLR)	1. Sampling frequencies apart from 12.8 kHz 2. 100% accuracy was achieved with a delay of 1/2 of a cycle 3. Precision rate up to 99%	Classification accuracy is 100%
Ibrahim et al. [113]	230 kV, 50 Hz TCSC is midpoint of the transmission line	Currents and voltages waveforms	2 cycles	TLS-ESPRIT algorithm and ANNs	1. TLS-ESPRIT algorithm, which is a modified version of the rotational invariance technique ESPRIT algorithm 2. Back-propagation algorithm is used and two hidden layers applied in the network 3. The sampling rate is 512 samples per cycle 4. With two levels of neural networks, level 1 ANN is used to detect the fault and level 2; four neural networks are used to identify the faulted phase	Not mentioned

Table 4 continued

Reference	System used	Input used	Post-fault data (cycle)	Algorithm	Feature	Numerical Result
Pérez et al. [24]	500 kV, 864 km, 50 Hz	One phase of current signal	2 ms	Adaptive wavelet and Bayesian classification	1. The sampling frequency is 500 kHz 2. DWT decomposition level 3 3. Mother wavelet—Daubechies-4 (Db4) 4. It provides directional-zone protection 5. Current signals of roughly 2 ms are analysed to get the result 6. 5328 faults cases were evaluated for analysis	Fault classification accuracy—100%, detection accuracy—100%
Dash et al. [114]	300 km, 500 kV, 60 Hz, STATCOM installed at midpoint	One-end voltage and measured line current phasors	½ cycle	Cumulative sum (CUSUM) and fast discrete S transform (FDST)	1. The sampling rate is 3.84 kHz 2. Spectral energy is extracted from current signal 3. No false detection has occurred during external faults even in the presence of high measurement noise 4. It is unaffected by the mutual coupling between the two lines	The fault location error is varying from 0.02 to 2.52%
Yadav et al. [18]	400 kV, 100-km, single-circuit transmission line 50 Hz	Three-phase current	1/4 cycle	WT and linear discriminant analysis (LDA).	1. Current signals are processed by WT up to level 3 2. Applicable for both single-circuit and double-circuit transmission line 3. Reach setting—99% of line length	For detection and classification accuracy—100%
Gupta et al. [115]	Static var compensator (SVC) transmission line 300 km, 400 kV, 50 Hz	Voltage and current signal at both ends	NA	Superimposed sequence components-based integrated impedance (SSCII).	1. The pilot-relaying schemes are suitable for with high-speed communication channels 2. Reliable for high as well as low resistance fault 3. Sampling frequency — 1 kHz	Fault detection time < 20 ms
Gopak umar et al. [116]	IEEE 14-bus 300 km, 400 kV generators on both sides, 50 Hz	Voltage and current phase angle		FFT analysis and support vector machine (SVM)	1. Single PMU used at only one of the generator buses used Park's transformation 2. 1300 samples have been utilized for training the SVM classifier 3. Sampling frequency of 10 kHz 4. PMU for synchronous measurements of voltage and current phasors	Fault classification accuracy—100%,

Table 4 continued

Reference	System used	Input used	Post-fault data (cycle)	Algorithm	Feature	Numerical Result
Swetapadma et al. [117]	400 kV, 50 Hz, the 100-km transmission line connected to infinite bus and IEEE 9-bus	Fundamental components currents and voltages and zero-sequence currents	½ cycle	Decision tree-based scheme	1. The advantage of the decision tree is that it is not affected by the size of the data set used for training 2. The reliability of this scheme is not affected by different fault conditions such as variation in fault type, fault distance, fault inception angle, fault resistance etc.	Accuracy of fault detection is 100% And overall accuracy of classification faults 99.9%
Moravej et al. [29]	250 kV, 300 km, 60 Hz	Current signal	½ cycle	S transform (ST) and probabilistic neural network (PNN) methods	1. Multilayered feedforward network having four layers such as the input layer, pattern layer, summation layer, the output layer 2. Input patterns through probability density function (PDF) apply to the second layer 3. The sampling frequency of three-phase current is 12 kHz 4. 780 cases are generated, i.e. 75% of this set is selected randomly to train PNN, and remaining data are used to test the process 5. The average accuracy for detection of power swing (C1) and fault during power swing (C2) is 95.5% and 90.93%, respectively	C1 and C2 are classified with accuracy 100 and 90%, respectively

of faults. The high-speed communication action is done by fibre-optic links/Etherne to locate the fault quickly, where PMU/digital fault recorder (DFR) is used as sampling unit.

9 Conclusions

Conventional methods are used for detection, classification and location of the fault in the transmission network, but to overcome the limitation of these methods, signal

Table 5 Comparative study of fault classification and location on transmission line

Reference	System used	Input used	Post-fault data (cycle)	Algorithm	Feature	Numerical result
Dash et al. [118]	230 kV, 50 Hz, 300 km and a TCSC located on a transmission line	Voltage and current signal	Not mentioned	Radial basis function neural networks (RBFNN) and fuzzy neural networks (FNN)	1. The activation function is Gaussian function 2. 50 data sets are used for training of the MRBFNN classifier and 140 data sets are used for FNN classifier. Similarly, for location 100 data sets considered for MRBFNN and 50 data set used for FNN	MRBFNN maximum location error = 5% and FNN maximum location error 8%
Joorabian et al. [38]	Abbaspor–Ahwaz-2 400 kV, 137 km, 50 Hz	Voltage and current signal	1 cycle	Radial basis function neural network (RBFNN)	1. The sampling frequency is 4 kHz 2. Total cases—3000 3. From total cases 60% cases are taken as training and other 40% used as testing data 4. 3000 training and testing sets are used for analysis	Fault location accuracy is $< 0.5\%$
Mahanty et al. [119]	100 km, three-phase, source voltage 400 kV	Three-phase currents and voltages	Not mentioned	Radial basis function (RBF) neural networks	1. Only current signals are required for fault classification 2. Wider range of (fault resistance) and fault inception angle used and compared to other schemes, and accuracy is good	Not mentioned
Gracia et al. [120]	La Lomba-Herrera single line network 380 kV, 189.3 km	Phase voltage and current values	Not mentioned	Artificial neural networks (ANNs)	1. ANN is carried out by means of a software tool called SARENEUR 2. Fault classification ANN has a linear activation function in the output layer more than two hidden layers and not more than six neurons per layer 3. Training time is less than a minute 4. Fault location ANN have two hidden layers (eight to nine neurons in the first layer and four to six in the second), nonlinear activation function in the input layer and linear activation function in the output layer 5. 15,352 number of cases are used 6. Villarino–Villalcampo double-circuit transmission line, 220 kV, 43.43 km is also tested	Classification errors are null in single lines and smaller than 1% in double-circuit lines Mean errors in the fault location oscillate between 0.015 and 0.4%

Table 5 continued

Reference	System used	Input used	Post-fault data (cycle)	Algorithm	Feature	Numerical result
Samantaray et al. [121]	400 kV, 300 km, 50 Hz	Current and voltage signal	2 cycle	Hyperbolic S transform (HS transform) and radial basis function neural network (RBFNN).	1. The sampling rate is 1.0 kHz 2. The feature (energy and standard deviation) is calculated by a change in one cycle ahead and one cycle back from the fault inception 3. RBFNN has been trained by 3000 sets of data 4. The error calculated for all kinds of faults is below 2% 5. RBFNN with recursive least quare (RLS) algorithm is used	Fault location error varies from 0.89 to 1.89%.
Reddy et al. [122]	400 kV, 300 km, 50 Hz	Three-phase voltages and currents	1 cycle	Wavelet transform and fuzzy inference system (FIS) and adaptive neuro-fuzzy inference system (ANFIS)	1. The triangular fuzzy number is implemented 2. Type-3 fuzzy reasoning and ANFIS architecture (type-3 ANFIS) is used 3. Sampling frequency of 12.5 kHz 4. The network is trained 3000 epochs for which error is about 3% 5. FIS editor (Mamadani type) MATLAB toolbox is used	Maximum fault location error varies − 3.67% to + 3.33%.
Samantaray et al. [123]	400 kV, 330 km, 50 Hz	Fault current and voltage signal	Not mentioned	Wavelet and SVM for classification and RBFNN (radial basis function neural network) with recursive least-square algorithm for location	1. Energy and standard deviation are extracted from the decomposed current signal 2. 'Haar' wavelet is applied as a mother function and decomposed up to third level 4. Radial basis function (RBF) kernel is used in SVM 5. SVM is trained with 120 sets of examples and tested for 300 data sets 6. The classification rate is 99.25% in the case of L–G fault which is the highest and least in the case of LLL–G fault bearing rate of 97.69% 7. RBFNN is trained by 3000 sets of data	Classification rates are above 97% and location error in all kinds of fault is below 2%

Table 5 continued

Reference	System used	Input used	Post-fault data (cycle)	Algorithm	Feature	Numerical result
Reddy et al. [44]	300 km, 400 kV	Current signal	Not mentioned	Wavelet neuro-fuzzy combined methods and adaptive neuro-fuzzy inference system (ANFIS)	1. For feature extraction from wavelet coefficient, FIS and ANFIS are used 2. Sampling rate—12.5 kHz 3. Mother wavelet — Daubechies (Db4) and decomposed up to 12th level by WT, but sixth level detail coefficients (d6) are considered in the analysis 4. Triangular fuzzy membership and Takagi–Sugeno's fuzzy controllers are used 5. ANFIS is using digital relaying applications in real time	Fault location maximum error of 6.5%
Bhalja et al. [124]	400 kV, 128 km, 50 Hz	Three-phase voltages and current signal	Not mentioned	Wavelet transforms and support vector machine classifier	1. 1000 fault data generation for data sets 2. Training data set = 4800 and testing data set = 1080 3. Sampling frequency = 80 samples/cycle 4. Db1 mother wavelet is applied	The Gaussian RBF kernel gives the highest accuracy of 98.5185%
Sadeh et al. [43]	220 kV, 50 Hz, Combined 90-km overhead and 10-km underground cable	Three-phase voltages and currents	1 cycle	ANFIS	1. Total training patterns—2132 2. Overhead line associated with—1520 patterns and rest patterns are for the underground cable 3. Rule base contains two fuzzy if–then rules of Takagi–Sugeno's type 4. Algorithm contains 10 ANFISs, 1 for fault type classification, 1 for faulty section detection, and the other 8 networks for accurate fault location (2 for each fault type)	Location maximum error is below 0.07% Fault classification overhead line maximum error is 0.0277 (24.9 m) and underground cable is 0.038(3.8 m)
Valsan et al. [125]	400 kV, 4 bus, 50 Hz	Three-phase current signals	<1 cycle	Wavelet transform	1. Relay gives directional protection 2. To detect the disturbance takes 1 ms 3. Total cases are 3750 4. Wavelet is decomposed up to only one level 5. Less computation burden and fast response	Fault location average error—0.217% and maximum absolute error < 3%

Table 5 continued

Reference	System used	Input used	Post-fault data (cycle)	Algorithm	Feature	Numerical result
Bhowmik et al. [34]	132 kV, 200 km, 50 Hz	Voltage and current signal	Not mentioned	DWT and BPNN	1. The signal is decomposed by DWT up to level three 2. The fault is detected around 20 ms 3. Training patterns—57 4. Testing (predicting) patterns—26	Not mentioned
Upender et al. [126]	400 kV, 50 Hz, 300 km	Three-phase line current signal	Not mentioned	Adaptive resonance theory (ART) neural network testing for classification and inverse interpolation method for fault location	1. Current signal decomposed into 9 levels using MRA algorithms 2. Db1 mother wavelet is used for classifying 10 types of fault 3. ART is capable of handling either binary or analogue input patterns/ samples 4. The multilayer perceptron neural network is used 5. 512(12.77 kHz) samples current signal 6. Total tested sample—1,209,600	Classification Accuracy = 99.91% and location errors, lower than 1.5%
Ya-Gang Zhang et al. [69]	IEEE 9-bus system and for IEEE 39	Voltage and current signal and power angle	Not mentioned	Pattern classification technology and WAMS	1. This paper presents real-time PMU measurements, we used mainly pattern classification technology and linear discrimination principle 2. The running time of discriminant analysis is 0.0320 s for IEEE 9-bus system 3. The running time of discriminant analysis is 0.0690 s for IEEE 39-bus system	Classification Accuracy = 100% for IEEE 9-bus system And for IEEE 39-bus classification Misjudgement ratio is 0.0256%
Dasgupta et al. [26]	220 kV, 150 km, 50 Hz, line/cable components (LCCs) of a pi network	Three-phase voltage signals	1 cycle	Wavelet packet, and neural network for Fault classification and Elman back-propagation Architecture for fault location	1. Mother wavelet is Daubechies Db4 2. The sampling frequency is 2000 samples per cycle 3. Signals are decomposed up to level 3 by WT 4. Test result—500 5. Pre-fault ½ cycle and post-fault ½ cycle of faulty	Fault distance estimate of 98.28% accurate and fault classifier accuracy of 98.67%

Table 5 continued

Reference	System used	Input used	Post-fault data (cycle)	Algorithm	Feature	Numerical result
Upendar et al. [127]	400 kV, 50 Hz. 300 km	Three-phase currets	Not mentioned	Classification and regression Tree (CART) and wavelet	1. CART is nonparametric in nature and does not require any variables to be selected in advance 2. CART algorithm will itself identify the most significant variables and eliminate non-significant one 3. CART results are invariant to monotone transformations of its independent variables 4. Wavelet decomposed three-phase current signal up to 7th level 5. A total of 1,209,600 fault cases were simulated	Classification accuracy is 99.88% and location error is less than 1.5%
da Silva et al. [128]	A 400 kV, 100-km-long transmission line	voltage and current signal	1 cycle	Stationary wavelet transform (SWT) and complex-domain neural networks	1. The 2000 samples per 60 Hz cycle 2. Daubechies' (Db4) mother wavelets are used 3. 152 fault scenarios are created for training the fault locators 4. 760 simulations are used for model validation and another 760 for testing 5. Mean absolute percentage errors (MAPEs) for the training, validation and test sets are less than 8% **for** a different model	Not mentioned
Dutta et al. [129]	IEEE 118-bus, parallel transmission line	Synchronized voltage and current signal	2 cycle	Synchronized voltage and current samples	1. The sampling frequency is 1 kHz 2. Detects and classifies faults within 7 ms for all types of faults 3. Comparing the change of sign of magnitudes of instantaneous power computed at two ends of a transmission line using synchronized voltage and current samples	Fault location accuracy is within 3%. Fault and classifier accuracy of 100%

Table 5 continued

Reference	System used	Input used	Post-fault data (cycle)	Algorithm	Feature	Numerical result
Yusuff et al. [130]	400 kV, 361.297 km, 50 Hz	Three-phase voltage and current signal	¼ cycle	Stationary wavelet transform (SWT), determinant function feature (DFF), support vector machine (SVM) and support vector regression (SVR)	1. Sampled at 3.2 kHz will give 64 samples per cycle 2. Approximation coefficient at level 5 for Haar, Db4 and Db6 wavelets are applied 3. In SVM, kernel function is used for better mapping in high-dimensional feature space 4. Fault inception angle varies 0°–90° 5. Support vector machine (SVM) and support vector regression (SVR) are used as classifier and regression, respectively	100% accuracy is achieved for classification and location accuracy is 2.10E−03
Yadav et al. [131]	400 kV, 200 km	Current and voltage signal	½ cycle	Fuzzy system	1. It is reliable, accurate and secure 2. Detect the fault (both forward and reverse) 3. Primary protection to 95% of line length 4. The fault location error is validated using Chi-square (χ^2) test	Fault location error—2%
Yadav et al. [31]	400 kV, 50 Hz, 300 km	Three-phase voltage and current	Not mentioned	Wavelet and artificial neural network	1. Db4 mother wavelet is decomposed to 3rd level of three-phase voltage and current 2. Average percentage error in fault location estimation is within 0.001% 3. Number of test case studies 10,000 cases 4. It offers primary protection to 99% of line length using single-end data only	% Error range in location Min. % error is 0.0007 and Max. % error is 0.6665

processing technique and artificial intelligence (AI)-based methods are widely applied in power system protection. Some of the selective and important papers are analysed to compare the system use, techniques, methods, input signal, features and numerical results, where artificial Intelligence (AI)-based method is the efficient, fast, accurate and robust

Table 6 Comparative study of fault classification, location and detection of transmission line

Reference	The system used	Input used	Post-fault data (cycle)	Algorithm	Feature	Numerical Result
Girgis et al. [132]	5-bus three-generator system	Current and voltage phasors	Not mentioned	Microprocessor-based protection that utilizes phasor quantity and artificial intelligence	1. The accuracy of fault location is good at relatively high impedance fault 2. Advancement in digital protection of power systems 3. The availability of communication links between different digital protection schemes	Not mentioned
Kezunovic et al. [133]	161 kV, 13.35 miles	Three-phase voltage and current samples	½ cycle	Synchronized sampling using global positioning system (GPS)	1. The minimum least-square method is applied for the location of the fault 2. Sampling frequency 24 kHz 3. The whole window of data contained 1 cycle of pre-fault and 2 cycles of post-fault data 4. Automated fault analysis is done by recording instrument	Fault location error less than 0.28%
Coury et al. [134]	400 kV, 330 km	Three-phase voltage and current samples	Not mentioned	Artificial neural network (ANN)	1. Alternative Transients Program (ATP) software was used 2. Error back-propagation (EBP) algorithm was utilized during the training process 3. The sampling frequency is 1 kHz 4. 4050 different faulted cases were applied 5. The training and validation sets are 80% and 20% of the total training set 6. Classification times between 4 and 12 ms	Fault detection takes 2 ms time and classification accuracy is 99.44%
Joe-Air Jiang et al. [135]	345 kV transposed transmission system	Synchronized voltage and current phasors	½ cycle	PMU phasors and fault detection index using Clarke transformation	1. EMTP/ATP simulator is adopted to evaluate 2. The sampling frequency is 1920 Hz (32 samples/cycle). 3. A total of 462 simulation studies have been conducted and 104 external fault is tested 4. Average fault detection time 1.624 ms	The average fault location error is well within 1%

Table 6 continued

Reference	The system used	Input used	Post-fault data (cycle)	Algorithm	Feature	Numerical Result
Zhang et al. [136]	345 kV, system section from CenterPoint Energy	Input voltage and current signals	1 cycle	Fuzzy adaptive resonance theory (ART) neural network and synchronized sampling	1. Fuzzy K-NN is used for classifying purpose 2. The sampling rate is 20 kHz 3. The data processing errors during calculation of phasors are avoided 4. It is tested also WECC 9-bus system	Maximum fault location error is 0.720 and 100% accuracy for detection
Roy et al. [137]	400 kV, 300-km-long three-phase transmission system	Three-phase voltage and current signal	Not mentioned	Computer-based digital relay algorithms using wavelet neuro-fuzzy techniques	1. The digital relay is based on combined approach of analytical hierarchy process (AHP) and fault tree analysis (FTA). 2. Wavelet coefficients of Db4 mother wavelet for the sixth level with a sampling frequency of 12.5 kHz 3. The standard fuzzy membership numbers called triangular fuzzy numbers are used	The acceptable failure rate varies from 0.01 to 0.316
Mohamed et al. [138]	High-Dam/ Cairo 500 kV, 788 km double-circuit line	Three-phase voltage and current samples	¼ cycle	ANN	1. The sampling rate was taken 16 samples per cycle of the power–frequency 2. Data window of 4 samples was utilized 3. The total number of samples is 9632 out of 70% use for training and 30% for testing 4. ANN is constructed from 24 input nodes, 24 hidden neurons and one output neuron	Not mentioned
Jiang et al. [48]	735 kV, 1000 km, 60 Hz	Three-phase voltage and current signal	1 cycle	SVM for fault classification and two-stage adaptive structure neural network (ASNNs) for fault location	1. Sampling rate-3860 Hz 2. Mother wavelet—Daubechies Db4 3. Current and voltage signal decomposed up to second level by multilevel DWT 4. IEEE 14-bus power network, fault detection accuracy—99.9%, fault classification, sensitivity and specification 99.73 and 99.9%, respectively	Average fault location error—0.61%

Table 6 continued

Reference	The system used	Input used	Post-fault data (cycle)	Algorithm	Feature	Numerical Result
Ibrahim et al. [139]	Egyptian 500 kV transmission network. 50 Hz	Three-phase voltage and line current	1 cycle	Nonlinear high impedance earth faults (HIEFs) using wavelet transform	1. Daubechies mother wavelet family (Db4) is used 2. The sampling rate employed is 12,500 Hz 3. Accurate faulty line determined at 0.04 s 4. Only used the RMS values, so synchronizing transmitted data are not needed	The error does not exceed 5%
Jiang et al. [140]	Taipower 345 kV power transmission network and total length of the power transmission lines is 939.61 km,	Three-phase voltage and current signal	1 cycle	Negative-sequence component (NSC), wavelet transform (WT), principal component analysis (PCA), support vector machines (SVMs), and adaptive structural neural networks (ASNNs)	1. Real-time power system simulator using field-programmable gate array (FPGA) platform 2. External cables at a sampling rate of 3840 samples per second are used to measure the signal 3. PCA module used 48 982 logic elements in the Stratix III FPGA. The maximum operating frequency is 76 MHz 4. There are 240,000 power signals generated for analysis 5. The response time of detecting a fault is around 0.0003 s 6. The averaged detection and sensitivity, accuracy is 99.9 and 99.87%, respectively	Classification accuracy is 99.78% and averaged fault location error is around 0.47%
Moravej et al. [47]	500 kV, 100 km, series compensation (SC) at midpoint and two ends of line	Voltage and current signal	1 cycle	Hyperbolic S transform (HS transform) and SVM	1. No need for fault section identification 2. District the internal and external faults 3. Extracting a characteristic feature (energy) from a half-cycle of the current waveform for the fault detection	1. Classification accuracy—99.21 2. District detection—98.11 3. Location relative error—2.48E−3

Table 6 continued

Reference	The system used	Input used	Post-fault data (cycle)	Algorithm	Feature	Numerical Result
Eristi et al. [141]	400 kV, 320-km, 50 Hz series compensated transmission line	Faulted voltage and current	1 cycle	Wavelet transform and adaptive neuro-fuzzy inference system	1. 23,436 fault cases, a data set is generated 2. Multiresolution analysis (MRA) is applied up to 6-level 3. The sampling frequency is 8 kHz 4. Db4 wavelet is chosen as the mother wavelet function 5. After feature extraction memory usage, size is reduced approximately 3200 times 6. The overall accuracy of fault section identification and classification is 99.187 and 99.301%, respectively	The fault location error is less than 0.25% on average
Roy et al. [35]	400 kV, 50-Hz, 300 km	Three-phase voltage and current signal	Not mentioned	S transform-based PNN classifier for fault classification and BPNN for fault localization	1. Training data set—1200 and testing data set—840 2. Gaussian noise 20 dB SNR is added in voltage and current signals 3. Due to noise in current signals, mean accuracy—98.7%. Fault location by BPNN has maximum error 4.46%	Fault classification average accuracy—99.6%
Krishnanand et al. 2015 [30]	400 kV, 308 km, 50 Hz	Phase current signal	1 cycle	CUSUM algorithm and 'Fast discrete S transform (FDST)'	1. CUSUM algorithm does the cumulative sum of the differences between the reference cycle and the present cycle to detect any sudden change in the signal amplitude 2. Sample size-640	Fault location error Min.—8.0986E−06, Max.—1.0269E−02
Shaik et al. [23]	500 kV, 500 MW, 60 Hz	Three-phase currents and voltage signal	½ cycle	Wavelet transforms Artificial neural networks	1. Sampled at a frequency of 1920 Hz 2. Current and voltage signals are processed by WT up to level 3 3. Bior4.4 mother wavelet is used to decompose three-phase voltages and current signal	Fault location Max. error—2.3%, Min. error—0.004%

Table 6 continued

Reference	The system used	Input used	Post-fault data (cycle)	Algorithm	Feature	Numerical Result
Dash et al. [142]	500 kV, 60 Hz, 230 km transmission line with static compensator (STATCOM)	Three-phase current signal at the sending end	1 cycle	Fast frequency filtering ST (FFST) along with a cumulative sum (CUSUM) average and fast Gauss–Newton (FGN) algorithm	1. Due to automatic frequency scaling technique reduces the computation 2. Sampling frequency —3.8 kHz 3. Fault detection and classification reliability > 97% high impedance faults (> 250 Ω) and 100% for low impedance faults	1. Fault classification time < 10 ms 2. Fault location accuracy—0.3%.
Esmaeilian et al. [143]	IEEE 118-bus system	Current and voltage signal at both ends of the bus	100 ms	Time-synchronized sampled data recorded by event-triggered intelligent electronic devices (IEDs)	1. The sampling rate was 96 samples per cycle for DFRs and 16 samples per cycle for DPRs 3. To detect relay misoperation 2. Computational burden as well as the required available post-fault data is reduced	For 108 cases where fault location error is less than 2.5%.
Hasheminejad et al. [144]	400 kV two paralleled line	Six current and six voltage signals at the sending end	Not mentioned	Intelligent travelling wave (TW)-based protection algorithm and fuzzy systems	1. The sampling frequency is 200 kHz 2. The Teager energy operator (TEO) is used to extract TWs from the signals 3. The faults are generated with the fault inception angles from 0° to 180° with the interval of 1.8° 4. The overall time elapsed for the internal fault identification and fault type classification is about 0.33 ms	1. The fault location error is 0.9% 2. With low inception angle and very accurate results

for detection, classification and location of the fault in a transmission line. This paper helps the researcher for development and further study in this field.

Compliance with ethical standards

Conflict of Interest The authors declare that there is no conflict of interests regarding the publication of this paper.

References

1. Lewis WA (1943) Principles of high-speed relaying. Westinghouse Eng 3:131–134
2. Crary SB (1947) Power system stability, vol 2. Wiley, New York
3. Hawary ME (1995) Electrical power systems. IEEE Press, New York, pp 469–536
4. IEEE guide for determining fault location on AC transmission and distribution lines (2005) IEEE Power Engineering Society Pub., New York, IEEE Std C 37.114
5. Magnago FH, Abur A (1999) Advanced techniques for transmission and distribution system fault location. In: Proceedings of CIGRE—Study committee 34 colloquium and meeting, Florence, paper 215
6. Capar A, Arsoy AB (2015) A performance oriented impedance based fault location algorithm for series compensated transmission lines. Electr Power Energy Syst 71:209–214
7. Eriksson L, Saha MM, Rockefeller GD (1985) An accurate fault locator with compensation for apparent reactance in the fault

resistance resulting from the remote—end feed. IEEE Trans Power Appar Syst 104:424–436
8. Takagi T, Yamakoshi Y, Yamaura M, Kondou R, Matsushima T (1982) Development of a new type fault locator using the one-terminal voltage and current data. IEEE Trans Power Appar Syst PAS-101(8):2892–2898
9. Novosel D, Bachmann B, Hart DG, Hu Y, Saha MM (1996) Algorithms for locating faults on series compensated lines using neural network and deterministic methods. IEEE Trans Power Deliv 11(4):1728–1736
10. Adu T (2001) A new transmission line fault locating system. IEEE Trans Power Deliv 16(4):498–503
11. Guobing S, Jiale S, Yaozhong G (2009) An accurate fault location algorithm for parallel transmission lines using one terminal data. Int J Electr Power Energy Syst 31(2–3):124–129
12. Sachdev M, Agarwal R (1988) A technique for estimating transmission line fault locations from digital impedance relay measurements. IEEE Trans Power Deliv 3(1):121–129
13. Girgis AA, Hart DG, Peterson WL (1992) A new fault location technique for two- and three-terminal lines. IEEE Trans Power Deliv 7(7):98–107
14. Dabbagh MA, Kapuduwage SK (2005) Using instantaneous values for estimating fault locations on series compensated transmission lines. Electr Power Syst Res 76(1–3):25–32
15. Dong X, Kong W, Cui T (2009) Fault classification and faulted phase selection based on the initial current travelling wave. IEEE Trans Power Deliv 24(2):552–559
16. Shehab-Eldin EH, McLaren PG (1998) Travelling wave distance protection-problem areas and solutions. IEEE Trans Power Deliv 3(3):894–902
17. Ngu EE, Ramar K (2011) A combined impedance and travelling wave based fault location method for multi-terminal transmission lines. Int J Electr Power Energy Syst 33(10):1767–1775
18. Yadav A, Swetapadma A (2015) A novel transmission line relaying scheme for fault detection and classification using wavelet transform and linear discriminant analysis. Ain Shams Eng J 6:199–209
19. Swetapadma A, Yadav A (2015) All shunt fault location including cross-country and evolving faults in transmission lines without fault type classification. Electr Power Syst Res 123:1–12
20. Silva KM, Souza BA, Brito NSD (2006) Fault detection and classification in transmission lines based on wavelet transform and ANN. IEEE Trans Power Deliv 21(4):2058–2063
21. Jung CK, Kim KH, Lee JB, Klockl B (2007) Wavelet and neuro-fuzzy based fault location for combined transmission systems. Electr Power Energy Syst 29:445–454
22. Valsan SP, Swarup KS (2008) Fault detection and classification logic for transmission lines using multi-resolution wavelet analysis. Electr Power Compon Syst 36:321–344
23. Shaik AG, Pulipaka RRV (2015) A new wavelet based fault detection, classification and location in transmission lines. Electr Power Energy Syst 64:35–40
24. Pérez FE, Orduña E, Guidi G (2011) Adaptive wavelets applied to fault classification on transmission lines. IET Gener Transm Distrib 5(7):694–702
25. Burrus CS, Gopinath RA (1998) Introduction to wavelets and wavelet transform: a primer. Prentice-Hall, Upper Saddle River
26. Dasgupta A, Nath S, Das A (2012) Transmission line fault classification and location using wavelet entropy and neural network. Electr Power Compon Syst 40:1676–1689
27. Mahari A, Seyedi H (2015) High impedance fault protection in transmission lines using a WPT-based algorithm. Electr Power Energy Syst 67:537–545
28. Ray P, Panigrahi BK, Senroy N (2013) Hybrid methodology for fault distance estimation in series compensated transmission line. IET Gener Transm Distrib 7(5):431–439
29. Moravej Z, Ashkezari JD, Pazok M (2015) An effective combined method for symmetrical faults identification during power swing. Electr Power Energy Syst 64:24–34
30. Krishnanand KR, Dash PK, Naeem MH (2015) Detection, classification, and location of faults in power transmission lines. Electr Power Energy Syst 67:76–86
31. Yadav A, Swetapadma A (2015) A single ended directional fault section identifier and fault locator for double circuit transmission lines using combined wavelet and ANN approach. Electr Power Energy Syst 69:27–33
32. Stockwell RG, Mansinha L, Lowe RP (1996) Localization of the complex spectrum: the S transform. IEEE Trans Signal Process 44:998–1001
33. Ekici S, Yildirim S, Poyraz M (2008) Energy and entropy-based feature extraction for locating fault on transmission lines by using neural network and wavelet packet decomposition. Expert Syst Appl 34:2937–2944
34. Bhowmik PS, Purkait P, Bhattacharya K (2009) A novel wavelet transform aided neural network based transmission line fault analysis method. Electr Power Energy Syst 31:213–219
35. Roy N, Bhattacharya K (2015) Detection, classification, and estimation of fault location on an overhead transmission line using S-transform and neural network. Electr Power Compon Syst 43(4):461–472
36. Mao KZ, Tan KC, Ser W (2000) Probabilistic neural network structure determination for pattern classification. IEEE Trans Neural Netw 11(4):1009–1016
37. Zhanga Jing-Ru, Zhanga Jun, Lokc Tat-Ming, Lyud Michael R (2007) A hybrid particle swarm optimization–back-propagation algorithm for feed forward neural network training. Appl Math Comput 185(2):1026–1037
38. Joorabian M, Asl SMAT, Aggarwal RK (2004) Accurate fault locator for EHV transmission lines based on radial basis function neural networks. Electr Power Syst Res 71:195–202
39. Gayathri K, Kumarappan N (2015) Double circuit EHV transmission lines fault location with RBF based support vector machine and reconstructed input scaled conjugate gradient based neural network. Int J Comput Intell Syst 8(1):95–105
40. Dash PK, Pradhan AK, Panda G (2000) A novel fuzzy neural network based distance relay scheme. IEEE Trans Power Deliv 15(3):902–907
41. Pradhan AK, Routray A, Pati S, Pradhan DK (2004) Wavelet fuzzy combined approach for fault classification of a series-compensated transmission line. IEEE Trans Power Deliv 19(4):1612–1618
42. Mendal JM (1995) Fuzzy logic systems for engineering: a tutorial. Proc IEEE 83(3):345–377
43. Sadeh J, Afradi H (2009) A new and accurate fault location algorithm for combined transmission lines using adaptive network-based fuzzy inference system. Electr Power Syst Res 79:1538–1545
44. Reddy MJ, Mohanta DK (2008) Adaptive-neuro-fuzzy inference system approach for transmission line fault classification and location incorporating effects of power swings. IET Gener Transm Distrib 2(2):235–244
45. Ekici S (2012) Support vector machines for classification and locating faults on transmission lines. Appl Soft Comput 12:1650–1658
46. Ray P, Mishra D (2016) Support vector machine based fault classification and location of a long transmission line. Eng Sci Technol Int J 19:1368–1380
47. Moravej Z, Khederzadeh M, Pazoki M (2012) New combined method for fault detection, classification, and location in series-

compensated transmission line. Electr Power Compon Syst 40:1050–1071
48. Jiang Joe-Air, Chuang Cheng-Long, Wang Yung-Chung, Hung Chih-Hung, Wang Jiing-Yi, Lee Chien-Hsing, Hsiao Ying-Tung (2011) A hybrid framework for fault detection, classification, and location—Part I: concept, structure, and methodology. IEEE Trans Power Deliv 26(3):1988–1998
49. Quinlan JR (1986) Induction of decision trees. Mach Learn 1(1):81–106
50. Esposito F, Malerba D, Semeraro GA (1997) A comparative analysis of methods for pruning decision trees. IEEE Trans Pattern Anal Mach Intell 19(5):476–491
51. Provost FJ, Domingos P (2003) Tree induction for probability-based ranking. Mach Learn 52(30):199–215
52. Liang H, Zhang H, Yan Y (2006) Decision trees for probability estimation: an empirical study. In: Proceedings of 18th IEEE international conference on tools with, artificial intelligence (ICTAI'06), pp 1–9
53. Malathi V, Marimuthu NS, Baskar S (2010) Intelligent approaches using support vector machine and extreme learning machine for transmission line protection. J Neuro Comput 73(10–12):2160–2167
54. Huang GB, Wang DH, Lan Y (2011) Extreme learning machines: a survey. Int J Mach Learn Cybern 2:107–122
55. Ray P, Mishra D (2014) Application of extreme learning machine for underground cable fault location. Int Trans Electr Energ. Syst. Published Online in Wiley Online Library, Dec. 2014
56. Mazon AJ, Zamora I, Miñambres JF, Zorrozua MA, Barandiaran JJ, Sagastabeitia K (2000) A new approach to fault location in two-terminal transmission lines using artificial neural networks. Electr Power Syst Res 56:261–266
57. Radojević ZM, Terzija VV, Djuric MB (2000) Numerical algorithm for overhead lines arcing faults detection and distance and directional protection. IEEE Trans Power Deliv 15(1):31–37
58. Chen Z, Maun Jean-Claud (2000) Artificial neural network approach to single-ended fault locator for transmission lines. IEEE Trans Power Syst 15(1):370–375
59. Funabashi T, Otoguro H, Mizuma Y, Dube L, Ametani A (2000) Digital fault location for parallel double-circuit multi-terminal transmission lines. IEEE Trans Power Deliv 15(2):531–537
60. de Morais Pereira CE, Zanetta LC (2004) Fault location in transmission lines using one-terminal post fault voltage data. IEEE Trans Power Deliv 19(2):570–575
61. Liao Y (2006) Fault location utilizing unsynchronized voltage measurements during fault. Electr Power Compon Syst 34:1283–1293
62. Jung H, Park Y, Han M, Lee C, Park H, Shin M (2007) Novel technique for fault location estimation on parallel transmission lines using wavelet. Electr Power Energy Syst 29:76–82
63. Reddy MJB, Mohanta DK (2008) Performance evaluation of an adaptive-network-based fuzzy inference system approach for location of faults on transmission lines using Monte Carlo simulation. IEEE Trans Fuzzy Syst 16(4):909–919
64. Perera N, Rajapakse AD (2008) Fast isolation of faults in transmission systems using current transients. Electr Power Syst Res 78:1568–1578
65. Gayathri K, Kumarappan N (2010) Accurate fault location on EHV lines using both RBF based support vector machine and SCALCG based neural network. Expert Syst Appl 37:8822–8830
66. Sadeh J, Adinehzadeh A (2010) Accurate fault location algorithm for transmission line in the presence of series connected FACTS devices. Electr Power Energy Syst 32:323–328
67. Ezquerra J, Valverde V, Mazoń AJ, Zamora I, Zamora JJ (2011) Field programmable gate array implementation of a fault location system in transmission lines based on artificial neural networks. IET Gener Transm Distrib 5(2):191–198
68. da Silva PRN, Negrão MMLC, Junior PV, Sanz-Bobi Miguel A (2012) A new methodology of fault location for predictive maintenance of transmission lines. Electr Power Energy Syst 42:568–574
69. Zhang Y, Wang Z, Zhang J, Ma J (2011) Fault localization in electrical power systems: a pattern recognition approach. Electr Power Energy Syst 33:791–798
70. Montañés M, García-Gracia A, El Halabi N, Comech MP (2012) High resistive zero-crossing instant faults detection and location scheme based on wavelet analysis. Electr Power Syst Res 92:138–144
71. Jiang Q, Li X, Wang B, Wang H (2012) PMU-based fault location using voltage measurements in large transmission networks. IEEE Trans Power Deliv 27(3):1644–1652
72. Mamis MS, Arkan M, Keles C (2013) Transmission lines fault location using transient signal spectrum. Electr Power Energy Syst 53:714–718
73. Mahamedi B, Zhu JG (2014) Unsynchronized fault location based on the negative-sequence voltage magnitude for double-circuit transmission lines. IEEE Trans Power Deliv 29(4):1901–1908
74. Dobakhshari AS, Ranjbar AM (2015) A novel method for fault location of transmission lines by wide-area voltage measurements considering measurement errors. IEEE Trans Smart Grid 6(2):874–884
75. Dalstein T, Kulicke B (1995) Neural network approach to fault classification for high speed protective relaying. IEEE Trans Power Deliv 10(2):1002–1011
76. Song YH, Xuan QX, Johns AT (1997) Comparison studies of five neural network based fault classifiers for complex transmission lines. Electr Power Syst Res 43:125–132
77. Aggarwal RK, Xuan QY, Dunn RW, Johns AT, Bennett A (1999) A novel fault classification technique for double-circuit lines based on a combined unsupervised/supervised neural network. IEEE Trans Power Deliv 14(4):1250–1256
78. Lin W-M, Yang C-D, Lin J-H, Tsay M-T (2001) A fault classification method by RBF neural network with OLS learning procedure. IEEE Trans Power Deliv 16(4):473–477
79. Adu T (2002) An accurate fault classification technique for power system monitoring devices. IEEE Trans Power Deliv 17(3):684–690
80. Youssef OAS (2004) Combined fuzzy-logic wavelet-based fault classification technique for power system relaying. IEEE Trans Power Deliv 19(2):582–589
81. Das B, Reddy JV (2005) Fuzzy-logic-based fault classification scheme for digital distance protection. IEEE Trans Power Deliv 20(2):609–616
82. Megahed AI, Moussa AM, Bayoumy AE (2006) Usage of wavelet transform in the protection of series-compensated transmission lines. IEEE Trans Power Deliv 21(3):1213–1221
83. Mahanty RN, Gupta PBD (2006) Comparison of fault classification methods based on wavelet analysis and ANN. Electr Power Compon Syst 34:47–60
84. Mahanty RN, Dutta Gupta PB (2007) A fuzzy logic based fault classification approach using current samples only. Electr Power Syst Res 77:501–507
85. Samantaray SR, Dash PK (2008) Transmission line distance relaying using machine intelligence technique. IET Gener Transm Distrib 2(1):53–61
86. Samantaray SR, Dash PK (2008) Pattern recognition based digital relaying for advanced series compensated line. Electr Power Energy Syst 30:102–112

87. Valsan SP, Swarup KS (2009) High-speed fault classification in power lines: theory and FPGA-based implementation. IEEE Trans Ind Electron 56(5):1793–1800
88. Nguyen T, Liao Y (2010) Transmission line fault type classification based on novel features and neuro-fuzzy system. Electr Power Compon Syst 38:695–709
89. Upendar J, Gupta CP, Singh GK, Ramakrishna G (2010) PSO and ANN-based fault classification for protective relaying. IET Gener Transm Distrib 4(10):1197–1212
90. Chothani NG, Bhalja BR, Parikh UB (2011) New fault zone identification scheme for busbar using support vector machine. IET Gener Transm Distrib 5(10):1073–1079
91. Seyedtabaii S (2012) Improvement in the performance of neural network-based power transmission line fault classifiers. IET Gener Transm Distrib 6(8):731–737
92. Beg MA, Khedkar MK, Paraskar SR, Dhole GM (2013) Feed-forward artificial neural network-discrete wavelet transform approach to classify power system transients. Electr Power Compon Syst 41:586–604
93. Jafarian P, Sanaye-Pasand M (2013) High-frequency transients-based protection of multiterminal transmission lines using the SVM technique. IEEE Trans Power Deliv 28(1):188–196
94. Vyas B, Maheshwari RP, Das B (2014) Investigation for improved artificial intelligence techniques for thyristor-controlled series compensated transmission line fault classification with discrete wavelet packet entropy measures. Electr Power Compon Syst 42(6):554–566
95. He Z, Lin S, Deng Y, Li X, Qian Q (2014) A rough membership neural network approach for fault classification in transmission lines. Electr Power Energy Syst 61:429–439
96. Vyas BY, Maheshwari RP, Das B (2014) Improved fault analysis technique for protection of Thyristor controlled series compensated transmission line. Electr Power Energy Syst 55:321–330
97. Gao F, Thorp James S, Gao S, Pal A, Vance KA (2015) A voltage phasor based fault-classification method for phasor measurement unit only state estimator output. Electr Power Compon Syst 43:22–31
98. Barros J, Drake JM (1994) Realtime fault detection and classification in power systems using microprocessors. IEE Proc Gem Transm Distrib 141(4):315–322
99. Liang J, Elangovan S, Devotta JBX (1998) A wavelet multi resolution analysis approach to fault detection and classification in transmission lines. Electr power Energy Syst 20(5):327–332
100. Chowdhury FN, Aravena JL (1998) A modular methodology for fast fault detection and classification in power systems. IEEE Trans Control Syst Technol 6(5):623–634
101. Wang H, Keerthipala WWL (1998) Fuzzy-neuro approach to fault classification for transmission line protection. IEEE Trans Power Deliv 13(4):1093–1104
102. Hong C, Elangovan S (2000) A B-spline wavelet based fault classification scheme for high speed protection relaying. Electr Mach Power Syst 28:313–324
103. Dash PK, Pradhan AK, Panda G (2001) Application of minimal radial basis function neural network to distance protection. IEEE Trans Power Deliv 16(1):68–74
104. Martín F, Aguado JA (2003) Wavelet-based ANN approach for transmission line protection. IEEE Trans Power Deliv 18(4):1572–1574
105. Yeo SM, Kim CH, Hong KS, Lim YB, Aggarwal RK, Johns AT, Choi MS (2003) A novel algorithm for fault classification in transmission lines using a combined adaptive network and fuzzy inference system. Electr Power Energy Syst 25:747–758
106. Chanda D, Kishore NK, Sinha AK Identification and classification of faults on transmission lines using wavelet multiresolution analysis. Electr Power Compon Syst 32:391–405
107. Chanda D, Kishore NK, Sinha AK (2005) Application of wavelet multiresolution analysis for identification and classification of faults on transmission lines. Electr Power Syst Res 73:323–333
108. Aguilera C, Orduna E, Ratta G (2006) Fault detection, classification and faulted phase selection approach based on high-frequency voltage signals applied to a series-compensated line. IEE Proc-Gener Transm Distrib 153(4):469–475
109. Zhang N, Kezunovic M (2007) Transmission line boundary protection using wavelet transform and neural network. IEEE Trans Power Deliv 22(2):859–869
110. Samantaray SR (2009) Decision tree-based fault zone identification and fault classification in flexible AC transmissions-based transmission line. IET Gener Transm Distrib 3(5):425–436
111. He Z, Fu L, Lin S, Bo Z (2010) Fault detection and classification in EHV transmission line based on wavelet singular entropy. IEEE Trans Power Deliv 25(4):2156–2163
112. Yusuff AA, Jimoh AA, Munda JL (2011) Determinant-based feature extraction for fault detection and classification for power transmission lines. IET Gener Transm Distrib 5(12):1259–1267
113. Ibrahim AM, Marei MI, Mekhamer SF, Mansour MM (2011) An artificial neural network based protection approach using total least square estimation of signal parameters via the rotational invariance technique for flexible AC transmission system compensated transmission lines. Electr Power Compon Syst 39:64–79
114. Dash PK, Moirangthem J, Das S (2014) A new time–frequency approach for distance protection in parallel transmission lines operating with STATCOM. Electr Power Energy Syst 61:606–619
115. Gupta OH, Tripathy M (2015) An innovative pilot relaying scheme for shunt-compensated line. IEEE Trans Power Deliv 30(3)
116. Gopakumar P, Reddy MJB, Mohanta DK (2015) Adaptive fault identification and classification methodology for smart power grids using synchronous phasor angle measurements. IET Gener Transm Distrib 9(2):133–145
117. Swetapadma A, Yadav A (2016) Data-mining-based fault during power swing identification in power transmission system. IET Sci Meas Technol 10(2):130–139
118. Dash PK, Pradhan AK, Panda G (2003) Application of artificial intelligence techniques for classification and location of faults on thyristor-controlled series-compensated line. Electr Power Compon Syst 31:241–260
119. Mahanty RN, Dutta Gupta PB (2004) Application of RBF neural network to fault classification and location in transmission lines. IEE Proc. Gener Transm Distrib 151(2):201–2012
120. Gracia J, Mazón AJ, Zamora I (2005) Best ANN structures for fault location in single and double-circuit transmission lines. IEEE Trans Power Deliv 20(4):2389–2395
121. Samantaray SR, Dash PK, Panda G (2006) Fault classification and location using HS-transform and radial basis function neural network. Electr Power Syst Res 76:897–905
122. Reddy MJ, Mohanta DK (2007) A wavelet-neuro-fuzzy combined approach for digital relaying of transmission line faults. Electr Power Compon Syst 35:1385–1407
123. Samantaray SR, Dash PK, Panda G (2007) Distance relaying for transmission line using support vector machine and radial basis function neural network. Electr Power Energy Syst 29:551–556
124. Bhalja B, Maheshwari RP (2008) Wavelet-based fault classification scheme for a transmission line using a support vector machine. Electr Power Compon Syst 36:1017–1030
125. Valsan SP, Swarup KS (2009) Wavelet transform based digital protection for transmission lines. Electr Power Energy Syst 31:379–388

126. Upendar J, Gupta CP, Singh GK (2010) Fault classification scheme based on the adaptive resonance theory neural network for protection of transmission lines. Electr Power Compon Syst 38:424–444
127. Upendar J, Gupta CP, Singh GK (2012) Statistical decision-tree based fault classification scheme for protection of power transmission lines. Electr Power Energy Syst 36:1–12
128. da Silva APA, Lima ACS, Souza SM (2012) Fault location on transmission lines using complex-domain neural networks. Electr Power Energy Syst 43:720–727
129. Dutta P, Esmaeilian A, Kezunovic M (2014) Transmission-line fault analysis using synchronized sampling. IEEE Trans Power Deliv 29(2):942–950
130. Yusuff AA, Jimoh AA, Munda JL (2014) Fault location in transmission lines based on stationary wavelet transform, determinant function feature and support vector regression. Electr Power Syst Res 110:73–83
131. Yadav A, Swetapadma A (2015) Enhancing the performance of transmission line directional relaying, fault classification and fault location schemes using fuzzy inference system. IET Gener Transm Distrib 9(6):580–591
132. Girgis AA, Johns MB (1989) A hybrid expert system for faulted section identification, fault type classification and selection of fault location algorithms. IEEE Trans Power Deliv 4(2):978–985
133. KezunoviC M, PeruniEiC B (1996) Automated transmission line fault analysis using synchronized sampling at two ends. IEEE Trans Power Syst 11(1):441–447
134. Coury DV, Oleskovicz M, Aggarwal RK (2002) An ANN routine for fault detection, classification, and location in transmission lines. Electr Power Compon Syst 30:1137–1149
135. Jiang Joe-Air, Chen Ching-Shan, Liu Chih-Wen (2003) A new protection scheme for fault detection, direction discrimination, classification, and location in transmission lines. IEEE Trans Power Deliv 18(1):34–42
136. Zhang N, Kezunovic M (2007) A real time fault analysis tool for monitoring operation of transmission line protective relay. Electr Power Syst Res 77:361–370
137. Roy DS, Mohanta DK, Panda AK (2008) Software reliability allocation of digital relay for transmission line protection using a combined system hierarchy and fault tree approach. IET Softw 2(5):437–445
138. Mohamed EA, Talaat HA, Khamis EA (2010) Fault diagnosis system for tapped power transmission lines. Electr Power Syst Res 80:599–613
139. Ibrahim DK, Saleh SM (2011) Unsymmetrical high-impedance earth fault central relay for transmission networks. Electr Power Compon Syst 39:1469–1492
140. Jiang J, Chuang C, Wang Y, Hung C, Wang J, Lee C, Hsiao Y (2011) A hybrid framework for fault detection, classification, and location—Part II: implementation and test results. IEEE Trans Power Deliv 26(3):1999–2008
141. Eristi H (2013) Fault diagnosis system for series compensated transmission line based on wavelet transform and adaptive Neuro-fuzzy inference system. Measurement 46:393–401
142. Dash PK, Das S, Moirangthem J (2015) Distance protection of shunt compensated transmission line using a sparse S-transform. IET Gener Transm Distrib 9(12):1264–1274
143. Esmaeilian A, Popovic T, Kezunovic M (2015) Transmission line relay mis-operation detection based on time-synchronized field data. Electr Power Syst Res 125:174–183
144. Hasheminejad S, Seifossadat SG, Razaz M, Joorabian M (2016) Traveling-wave-based protection of parallel transmission lines using Teager energy operator and fuzzy systems. IET Gener Transm Distrib 10(4):1067–1074
145. Martinez AM, Kak AC (2001) PCA versus LDA. IEEE Trans Pattern Anal Mach Intell 23:228–233
146. Thukaram D, Khincha HP, Vijaynarasimha HP (2005) Artificial neural network and support vector machine approach for locating faults in radial distribution systems. IEEE Trans Power Deliv 20:710–721
147. Nazari-Heris M, Mohammadi-Ivatloo B (2015) Application of heuristic algorithms to optimal PMU placement in electric power systems: an updated review. Renew Sustain Energy Rev 50:214–228
148. Korkali M, Lev-Ari H, Abur A (2012) Traveling-wave-based fault-location technique for transmission grids via wide-area synchronized voltage measurement. IEEE Trans Power Syst 27:1003–1011
149. Korkali M, Abur A (2013) Optimal deployment of wide-area synchronized measurements for fault-location observability. IEEE Trans Power Syst 28:482–489
150. Azizi S, Sanaye-Pasand M (2015) A straightforward method for wide-area fault location on transmission networks. IEEE Trans Power Deliv 30:264–272
151. Salehi-Dobakhshari A, Ranjbar AM (2014) Application of synchronised phasor measurements to wide-area fault diagnosis and location. IET Gener Transm Distrib 8:716–729
152. Jiang JA, Chen CS, Liu CW (2003) A new protection scheme for fault detection, direction discrimination, classification, and location in transmission lines. IEEE Trans Power Deliv 18:34–42
153. Asuhaimi Mohd Zin A, Saini M et al (2015) New algorithm for detection and fault classification on parallel transmission line using DWT and BPNN based on Clarke's transformation. Neurocomputing 168:983–993
154. Jutten C, Herault J (1991) Blind separation of sources, part I: AN adaptive algorithm based on neuromimetic architecture. Signal Process 24:1–10
155. Comon P (1994) Independent component analysis a new concept. Signal Process 36:287–314
156. Almeidaa AR, Almeidaa OM, Juniora BFS, Barretob LHSC, Barros AK (2017) ICA feature extraction for the location and classification of faults in high-voltage transmission lines. Electr Power Syst Res 148:254–263
157. Cichocki A, Amari S (2003) Adaptive blind signal and image processing. Wiley, New York
158. Hyvarinen A, Karhunen J, Oja E (2001) Independent component analysis. Wiley-Interscience, New York
159. Hua Y, Sarkar TK (1990) Matrix Pencil method for estimating parameters of exponentially damped/undamped sinusoids in noise. IEEE Trans Acoust Speech Signal Process 38(5):814–824
160. Hua Y, Sarkar TK (1991) On SVD for estimating generalized eigenvalues of singular matrix Pencil in noise. IEEE Trans Signal Process 39(4):892–900
161. Wang L, Suonan J, Jiao Z (2013) A fast extraction method in the application of UHV transmission line fault location. Energy Power Eng 5:1277–1283
162. Sarkar TK, Pereira O (1995) Using the matrix pencil method to estimate the parameters of a sum of complex exponentials. IEEE Antennas Propag Mag 37(1):48–55
163. Hua Y, Sarker TK (1988) Matrix pencil method and its performance. Acoust Speech Signal Process 4:2476–2479
164. Lopes FV, Silva KM, Costa FB, Neves WLA, Fernandes D (2015) Real-time traveling-wave-based fault location using two-terminal unsynchronized data. IEEE Trans Power Deliv 30(3):1067–1076
165. Pignati M, Zanni L, Romano P, Cherkaoui R, Paolone M (2017) Fault detection and faulted line identification in active distribution networks using synchrophasors-based real-time state estimation. IEEE Trans Power Deliv 32(1):381–392

166. Silveira EG, Pereira C (2007) Transmission line fault location using two-terminal data without time synchronization. IEEE Trans Power Syst 22(1):498–499
167. Costa FB, Souza BA, Brito NSD (2010) Real-time detection of fault-induced transients in transmission lines. Electron Lett 46(11)
168. Bouthiba T (2004) Fault location in EHV transmission lines using artificial neural networks. Int J Appl Math Comput Sci 14(1):69–78
169. Costa FB, Souza BA (2011) Fault-induced transient analysis for real-time fault detection and location in transmission lines. In: International conference on power systems transients (IPST'11) in Delft, Netherlands, June 2011, pp 1–6
170. Costa FB, Souza BA, Brito NSD (2012) Real-time classification of transmission line faults based on maximal overlap discrete wavelet transform. PES T&D 2012, pp 1–8